

**GOLD NANOPARTICLE MEDIATED MEMBRANE
PERMEABILIZATION OF PHYTOCHEMICALS INTO
BREAST CANCER CELLS**

A Thesis presented to
the Faculty of the Graduate School
at the University of Missouri

In Partial Fulfillment
of the Requirements for the Degree of
Master of Science

by

FEIFEI CHEN

Dr. John Viator, Thesis Supervisor

May 2014

The undersigned, appointed by the Dean of the Graduate School, have examined the thesis entitled:

GOLD NANOPARTICLE MEDIATED MEMBRANE
PERMEABILIZATION OF PHYTOCHEMICALS INTO BREAST
CANCER CELLS

presented by Feifei Chen,

a candidate for the degree of Master of Science

and hereby certify that, in their opinion, it is worthy of acceptance.

Dr. John Viator, Bioengineering

Dr. Gang Yao, Bioengineering

Dr. Gregory Triplett, Electrical and Computer Engineering

ACKNOWLEDGMENTS

I would like to acknowledge Dr. Viator for all his help and mentoring through the two and a half years that I have been here in VIATOR Lab. He provided me opportunities when I first came to America, to University of Missouri. He made me learn how to study a problem and solve the problem. More importantly, he encouraged me all the time even though I just got only a little result in the research. I really appreciate for his support and much more. I cannot go on without also thanking Dr. Yao and Dr. Triplett for being on my committee and providing me with much needed guidance.

I would also like to thank the members of the VIATOR Lab who have helped me countless number of times, especially Kiran Bhattacharyya, Ben Goldschmidt and Paul Whiteside. Each time I faced a problem, they would like to discuss with me and give me suggestions. Without their help, I would never successfully get data I wanted and would never overcome research frustrations. Moreover, since I'm not a native English speaker, they were so patient to explain things to me and even helped to improve my speaking English.

I would like to thank my boyfriend Jiazhen Zhou and my best friends here in America, Molly McCormick and Yiyi Li, who accompanied me each time when I was frustrated with research. Thanks to their moral support and love, I could vent research pressure and insist on completing this thesis.

Finally, I would like to acknowledge my parents, Hen'an Chen and Ronglan Mao. Without them everything would be meaningless. They love me so much and encourage me all the time. They supported me to go abroad and chase my dream, even though they miss me so much but haven't seen me for over one year.

There are undoubtedly others who have not mentioned here, but I am grateful for everyone who helped me come this far. What they've done for me have made me who I am today and given me confidence to keep on working hard in the next journey.

TABLE OF CONTENTS

ACKNOWLEDGMENTS	ii
LIST OF TABLES	vii
LIST OF FIGURES	viii
ABSTRACT	x
Chapter	
1. INTRODUCTION	1
1.1 Breast Cancer	1
1.2 Anti-cancer Phytochemicals	3
1.2.1 β -Carotene	4
1.2.2 Lycopene	7
1.2.3 Curcumin	10
1.3 Biomedical Optics	12
2. MATERIALS AND METHODS	20
2.1 Materials	20
2.1.1 Cell Culture	20
2.1.2 Reagents	20
2.1.3 Equipment	21
2.2 Experimental Methods	21
2.2.1 Pretreatment of Conjugation of Au NPs and Breast Cancer Cells	21
2.2.2 Optoporation	23
2.2.3 Cell Permeabilization Confirmation by Fluorescent Test	24
2.2.4 β -Carotene/PEG Test	26

2.2.5 Control Groups Test	27
2.2.5.1 Absorption of Laser Treatment Solutions	27
2.2.5.2 Cells with Membrane-bound Au NPs and Incubate with 1 × PBS	28
2.2.5.3 Cells without Membrane-bound Au NPs and Incubate with PEG	28
2.2.6 β -Carotene/DPPC Liposomes Test	28
2.2.7 Tetracycline as the Laser Treatment Solution	29
3. RESULTS	30
3.1 Cell Death Caused by PEG Solutions in the Absence of β -Carotene	30
3.2 Cell Death Caused by PEG Solutions in the Presence of β -Carotene	34
3.3 Results of Control Groups	38
3.3.1 Confirmation of Light Absorbance of Treatment Solutions	38
3.3.2 Impact of Cells with Au NPs Suspended in 1 × PBS	39
3.3.3 Impact of Cells without Membrane-bounded Au NPs Suspended in PEG Solutions	39
3.4 Influence of β -Carotene/DPPC Liposomes on Irradiated Cells	40
3.5 Influence of Tetracycline on Irradiated Cells	41
4. DISCUSSION	43
4.1 Comparison between PEG200 and PEG400 in the Absence/Presence of β -Carotene	43
4.2 β -Carotene/DPPC Liposomes as Anti-cancer Drug.....	46
4.3 Tetracycline as Anti-cancer Drug	46
5. CONCLUSION	48
APPENDIX	49
A Calculations of Cell Death by ImageJ	49

BIBLIOGRAPHY	50
VITA	55

LIST OF TABLES

Table	Page
3.1 Cell Death from PEG200	32
3.2 Cell Death from PEG400	34
3.3 Cell Death from β -Carotene/PEG200	37
3.4 Cell Death from β -Carotene/PEG400	37

LIST OF FIGURES

Figure	Page
1.1 Possible Photoacoustic Wave Emitted by Sample	13
1.2 Exponential Decay of Light in Medium as Function of Path Length	14
2.1 Principle Conjugation of Au NPs and T47D Cells	22
2.2 Experimental Equipment and Area Exposed to Laser	24
2.3 Cell Permeability Proved by Fluorescence Stain	25
3.1 Increasing Cell Permeability from PEG200 in Irradiated Area	30
3.2 Increasing Cell Permeability from PEG200 in Non-irradiated Area	31
3.3 Plot of Cell Death Suspended in PEG200	32
3.4 Increasing Cell Permeability from PEG400	33
3.5 Plot of Cell Death Suspended in PEG400	34
3.6 Increasing Cell Permeability from β -Carotene/PEG200	35
3.7 Plot of Cell Death Suspended in β -Carotene/PEG200	36
3.8 Increasing Cell Permeability from β -Carotene/PEG400	36
3.9 Plot of Cell Death Suspended in β -Carotene/PEG400	37
3.10 Absorbance of Treatment Solutions	38
3.11 Fluorescence Image of Cells Suspended in PBS	39
3.12 Fluorescence Image of Cells without Membrane-bound Au NPs Suspended in PEG Solutions	40
3.13 Fluorescence Image of Cells Suspended in β -Carotene/DPPC Liposomes	41
3.14 Cell Non-viability by Tetracycline and Stained by Trypan Blue	42
4.1 Comparison of Cell Death Resulted from PEG200 and PEG400	43

4.2 Comparison of Cell Death Resulted from β -Carotene/PEG200 and β -Carotene/ PEG400	44
4.3 Comparison of Cell Death Resulted from β -Carotene/PEG200 and PEG200	45
4.4 Comparison of Cell Death Resulted from β -Carotene/PEG400 and PEG400	45
A.1 Fluorescence Image of Cells Suspended in β -Carotene/PEG200 in Irradiated Area..	49

GOLD NANOPARTICLE MEDIATED MEMBRANE PERMEABILIZATION OF PHYTOCHEMICALS INTO BREAST CANCER CELLS

Feifei Chen

Dr. John A. Viator, Thesis supervisor

ABSTRACT

Breast cancer is one of the most common cancers in women with a very high incident rate, especially for those women who are between 40-60 years old. Most drugs are large or non-polar macromolecules, which cannot get into cancer cells autonomously, so a method that can deliver those drugs is very important. Optoporation method has been facilitated with gold nanoparticles, which are bound to breast cancer cells, and then absorb the optical energy to improve the membrane permeabilization. Long-term dietary consumption of fruits and vegetables high in β -carotene and other phytochemicals has been shown beneficial in terms of anti-cancer, anti-aging, preventing cardiovascular disease and cataract. However they are large non-polar molecules that are difficult to enter the cancer cells. Here in this study, we applied optoporation method by using β -carotene, and tetracycline as anti-cancer drugs in various concentrations to optimize highest selective cell death/best potential for T47D breast cancer cell lines.

Chapter 1

Introduction

1.1 Breast Cancer

Cancer is a type of disease that caused by the abnormal of cell proliferation. Aside from the out control of cell growth, those abnormal cells can invade other tissues around, or even other parts of the body via circulatory system or lymphatic system. Breast cancer is a kind of cancer that often happens in mammary glandular epithelium, also called lobules, and the milk ducts. ¹ According to Alteri et al, in 2011, worldwide, breast cancer comprises 22.9% of all cancers. About 230,480 women in the US suffer from invasive breast cancer and the number of women who die from breast cancer is around 39,520. ¹ Breast cancer does not result in death, but since the abnormal cells are free to transfer to other body sites and eventually develop life-threatening metastatic diseases. The most common sites are lung, liver, skin and bones. ² It happens much more often among women than men. Women who are 50 to 60 years old have higher risk to suffer from breast cancer. It strongly affects women's physical and psychological health and their lives. Therefore, effective breast cancer therapy is extremely important.

Current treatments include surgery, radiotherapy, endocrine, chemotherapy, and targeted therapy.

Breast cancer surgery plays an important role in diagnosing, assessing and systemic therapy. The aim of breast cancer surgery is to remove the lesion from breast. Usually, two kinds of surgeries, lumpectomy and mastectomy, are offered to patients. In a mastectomy, the entire breast has to be removed. Hence, patients have to consider the

breast reconstruction. Lumpectomy includes removal of only carcinomatous tissue.¹ But lumpectomy is very strict and cannot be used for all patients. For those who are not suitable to lumpectomy, mastectomy is still necessary.

Radiation is usually used after surgery. It is found that, for more than 41% patients, tumor cells still exist at a distance of about 2 cm from the lesion after lumpectomies.³ The goal of radiation is to destroy the remaining cancer cells in breast by radioactive rays. For advanced breast cancer, post-mastectomy irradiation is found to be highly effective since radiotherapy can minimize the tumor size.³ However, for early breast cancer patients, radiotherapy generally should not be used because of the side effects that it can damage human immune system.

Some patients are not suitable for surgery or radiotherapy. In this situation, endocrine therapy is often considered for those whose breast cancers test positive for endocrine receptors. Endocrine function can be modified by drugs or by the removal of endocrine gland, so that lower the estrogen level to control the breast cancer.¹ The amounts of drugs or method used in endocrine therapy depend on the menstruation. However, most breast cancers happen in women who are postmenopausal, hence, more therapies are needed.

In chemotherapy, doctors use anticancer drugs to stop cell division and destroy cancer cells. It is shown that adjuvant chemotherapy can reduce local recurrence by 30% and death by 20%.⁴ And when the full dose and cycle of drugs is completed in a well-timed manner, chemotherapy is most effective.¹ Side effects from this treatment include alopecia, nausea, diarrhea infertility and even myelosuppression,² which will result in much painful.

Targeted therapy has been studied a lot by researchers recently. Compare with chemotherapy, targeted therapy is new and more complicated that has many levels of actions. About 15%-30% of breast cancers overproduce the growth-promoting protein HER2/neu.¹ These tumors grow faster and are more likely to recrudescence. Clinically, trastuzumab, as a monoclonal antibody, is used to target the HER2 protein directly. Patients that overexpress HER2 get a survival benefit from trastuzumab.¹ Its main problem is cardiac failure, and it's toxicity when combining with anthracyclines. Instead of trastuzumab, other new drugs include the oral tyrosine kinase inhibitor, lapatinib, and the antiangiogenic drug, bevacizumab, have proved effectiveness and can be used in clinical.² However, not every patient can afford them because of the high cost.

Breast cancer is a significant problem in the world. Despite early diagnosis and treatment can make patients survive longer time, it is essential to develop further therapy and more novel methods that can improve survival from this cancer in worldwide.

1.2 Anti-cancer Phytochemicals

As discussed above, chemicals are generally used to inhibit the carcinogenesis of breast cancer. Cancer chemoprevention is represented as an effective method to control the process of carcinogenesis by the chemical compounds.⁵ With increasing evidence coupled with considerations of quality, safety, and efficacy, researchers found that phytochemical is a strategy to induce the cancer chemoprevention.⁶ Phytochemicals are chemical compounds that can be extracted from dietary and natural plants. They are usually non-nutrients but emerged as promising sources of antioxidants and new chemotherapy adjuvants, with the ability of anti-carcinogenesis and anti-mutagenesis.

The NCI has demonstrated that there are more than 1000 kinds of different phytochemicals found rich in vegetables, fruits and herbs, are capable to prevent cancer, such as curcumin in turmeric, genistein in soy beans, lycopene in tomatoes, sulphoraphane in broccoli.⁷

The relatively non-toxic phytochemicals, which are related to apoptosis and growth restraint of cancer cells, could block the occurrence of DNA mutation caused by carcinogenic substance. Phytochemicals possess their chemoprevention through the operation of phase I and phase II metabolic enzymes in tissues.⁸ During phase I metabolism, oxidation, reduction and hydrolysis of xenobiotics are the main reactions. Phase II metabolism also called as detoxifying metabolism. Carcinogens and activated phase I metabolites are combined with amino acids, glucuronic acid, or glutathione to produce water-soluble conjugates that are egested in bile or kidney.⁹ Many researches have been studied to explain the principle of chemopreventive property of phytochemical. Shu et al explained that, by some common signaling pathways, include using a leucine zipper transcription factor NF-E2-related factor 2 (Nrf2) and nuclear factor- κ B (NF- κ B) to mediate anti-oxidative stress effects, phytochemicals can block cancer initiation, induce apoptosis in tumor cells and even prevent tumor metastasis.⁹

1.2.1 β -Carotene

β -Carotene is a type of phytochemical and is abundant in fruits and vegetables. It is a member of carotenes, which can be found in carrots, sweet potatoes and pumpkins. β -Carotene is non-polar lipophilic compound. Hence the absorption of β -carotene is higher when eaten with fats. β -Carotene is the precursor of vitamin A. One molecule of β -

carotene can be cleaved into two molecules of vitamin A. Thus, β -carotene provides high rate of the vitamin A demand in diet. β -Carotene has influence on anticancer, anti-aging, preventing cardiovascular disease and cataract. Researchers found that long-term intake of fruits and vegetables high in β -carotene is related to lower risk of cancer.¹⁰ In vitro, researches showed that carotenoids inhibit cell division and growth of mutant cells.¹¹ However, the association between breast cancer and β -carotene are debatable. Two prospective cohort studies claimed opposite opinions on the relation between β -carotene consumption and breast cancer. One reported preventive effect,¹² one suggested no obvious relation.¹³ Paolo et al investigated the etiological aspect of breast cancer and β -carotene intake. In the case-control study involving 270 cases and 270 controls, β -carotene was examined in serum samples by using liquid chromatography. Their research showed that, when reducing serum concentrations of β -carotene, the risk of breast cancer increased obviously.¹⁴

On the other hand, Xiaoming et al demonstrated the oxidation products of β -carotene are associated with the inhibition of breast cancer. They isolated a mixture by oxidizing β -carotene through certain chemical methods. Then chemically characterized this mixture by HPLC-mass spectrometry and nuclear and magnetic resonance (NMR) spectroscopy. A fraction rich in oxidative products of β -carotene was added into breast cancer (MCF-7) cells to see the influence on cellular growth and metabolism in MCF-7 cells.¹⁵ Cell viability was determined by Trypan blue dye exclusion. In this way, they found that this fraction exceedingly prevents cell growth in MCF-7 cells. The oxidized fraction products of β -carotene reported in their work were not from oxidation of retinol or retinoic acid, and they cannot be replaced for retinoic acid in cotransfection assays. Also, they found

that butylated hydroxytoluene (BHT) keeps from inhibition of growth of MCF-7 cells by β -carotene. However, BHT doesn't protect against inhibition of growth by the oxidized products of β -carotene. Cells conjugated with mevalonate protect cells against inhibition of growth by the oxidized products of β -carotene. Contrarily, mevalonate does not prevent inhibition of growth by retinoic acid. In summary, they thought the oxidation products of β -carotene have potential anti-cancer activity.¹⁵

Many experiments about β -carotene have been done. Large numbers of tests reported that β -carotene kill cancer. However, some studies also showed that high doses of β -carotene result in greater risk of lung cancer for those current or former smokers.¹⁶ Researchers used to get data from 3 large groups of volunteers for meta-analysis. The result suggested a higher opportunity of lung cancer among smokers when taking β -carotene supplements.¹⁷

Robert et al used ferret to do the research about the association between the intake of β -carotene and lung cancer. Ferret mimics the human tissue metabolism of β -carotene. In addition, some researchers have used ferret for studies of tobacco smoking and inhalation toxicology.¹⁸ First, they gave ferrets a high-dose β -carotene supplement, and exposed them to cigarette smoke for six months. An obvious increasing response in lung tissue was observed in all β -carotene-supplemented animals. Moreover, this proliferative response was even stronger by exposure to tobacco smoke.¹⁹ On the other hand, authors also gave ferrets either physiological- or pharmacologic-dos β -carotene supplementation. The ferrets were treated with cigarette smoke also for six months. As a result, they found the retinoic acid concentration was decreased in the lung tissues, while the expression of proliferative cell were greater in the animals of high-dose beta-carotene-supplementation

with or without smoke. The same result for the smoke-exposed animals with low-dose beta-carotene-supplemented. Here this situation doesn't include the low-dose beta-carotene-supplemented animals, as compared with the control trial. These results suggested that, compared with the pharmacologic dose of β -carotene, a physiologic dose of β -carotene in ferrets with exposure to smoke, has little harmful influence, and may protect themselves weakly against lung cancer caused by tobacco smoke.¹⁹

Also, they demonstrated the fact that researchers should focus on more other micronutrient combinations, which can be found abundantly in fruits and vegetables, rather than just be interested in the use of only single micronutrient. It may be specifically important to have more antioxidant defenses when taking high doses of β -carotene for the sake of preventing the production of carotene abnormal products, as well as the succeeding events that can result from them.¹⁹

1.2.2 Lycopene

Lycopene is a bright red pigment and is a type of phytochemical presents in many fruits and vegetables, especially red foods, such as tomatoes, guava and red bell peppers. So it is commonly found in the diet from dishes and absorbed by humans. Different with β -carotene, lycopene cannot be cleaved into vitamin A, even though it is a kind of carotenoids. As an extremely unsaturated and straight chain hydrocarbon, lycopene has eleven conjugated and two non-conjugated double bonds. In addition, it is unsolvable in water and can only be dissolved in oils or organic solvents. In vivo, lycopene can be absorbed through lipoproteins. On the other side, lycopene is also used in daily life very often as a stain because of its deep red color, non-polarity and non-toxicity.

Lycopene is also a strong antioxidant. Its ability to clear up free radical is much stronger than others. Many studies have showed that lycopene is associated with reduced risk of chronic diseases including cancer and heart diseases by protecting important molecules, such as lipids, proteins and DNA.²⁰ Its effective antioxidant is due to the great singlet oxygen quenching ability, which result from the large number of conjugated double bonds. Lycopene plays an essential role in protecting several human cancers.²⁰

In early study, researchers did experiments in mice and found chronic dietary consumption of lycopene obviously delayed the beginning of autonomous mammary tumors and reduced their growth and development. The reason why this result happened was because the activity of mammary gland thymidylate synthetase was decreased and serum free fatty acids and prolactin was reduced. Prolactin is a hormone that is associated with breast cancer development.²¹ Fornelli et al studied the affect of lycopene on the viability of the breast cancer cell line (MCF-7). Lycopene or its oxidative products have the ability to increase the expression of Connexin 43 (Cx43) at the protein levels in the human and mouse, hence, Gap Junction Intercellular Communication (GJIC) between preneoplastic and normal epithelial cells can be improved since connexins make up the Gap Junction Channels. Additionally, the GJCs help to deliver the growth inhibitory signals, which can prevent the development of abnormal cells.²² That is considered as the reason for lycopene protecting against breast cancer cells. Fornelli et al dissolved lycopene in tetrahydrofuran (THF) containing 0.25% butylated hydroxytoluene (BHT). They used two methods to test the influence of lycopene on MCF-7 cells, MTT assay and BrdU assay. Moreover, their experiment was time and dose-response.²³ They found when increasing the concentration of lycopene, cell non-viability was also increased.

Lycopene showed cytotoxic at the highest concentration. In addition, the experiments of cell non-viability caused by lycopene were also carried out depend on different exposure time. The results showed that cell non-viability was highest when exposure to 24 hours at 3 μ M lycopene. However, the number of dead cells were not linear increased when exposure longer time. As they reported, when exposed to 48 hours, cells containing lycopene formed a discontinuous monolayer, and the GJIC was inhibited and cell non-viability was not as high as 24 hours.

Therefore the time of 24-hour of lycopene treatment was chosen to perform dose–response experiments.²³ They also proved that the increase of GJIC seems to be completely induced by increasing lycopene concentration. Therefore lycopene induced the up regulation of Cx43 mRNA to increase expression of the connexin 43 genes. Those above data from Fornelli et al confirmed that lycopene can inhibit the growth of MCF cells and has influence on GJIC modulation.²³

Besides treating breast cancer, lycopene has been studied to treat other cancers in different papers.

Tang et al did some research about lycopene preventing human prostate cancer. Three different human prostate cancer cell lines, involving androgen-independent prostate DU145, PC-3 cancer cells and androgen-dependent prostate LNCaP cancer cells, were used to test the association between lycopene and prostate carcinoma. They found that lycopene inhibited the growth of all three prostate cancer cells but androgen-dependent LNCaP cells were less prevented than the other two cell lines. In addition, they found the DU145 and PC-3 cancer cell viabilities were related to concentration of lycopene and treatment time. Generally, cell viability is indirection proportion to time

and inversely proportional to concentration of lycopene. Their work proved that lycopene is a promising phytochemical for human prostate cancer chemoprevention.²⁴

Lycopene may have effect on other malignant cell lines besides breast cancer and prostate cancer cell lines. Salman et al examined the anti-cancer effect of lycopene on other carcinomatous cell lines, including human colon carcinoma (HuCC), B chronic lymphocytic leukemia (EHEB), human erythroleukemia (K562) and Raji, a prototype of Burkitt lymphoma cell line. Their results showed that lycopene obviously inhibited the growth of HUCC, K562 and Raji cell lines and the inhibition depends on the concentration of lycopene (1.0, 2.0, and 4.0 μM). On the other hand, EHEB cells were observed being prevented by lycopene only when lycopene was at its largest concentration.²⁵

In summary, many studies have been examined to test anti-proliferative effect of lycopene on different types of cancers, including breast cancer and prostate cancer,^{23, 24} which have been proved previously, HuCC and Raji cell lines.²⁵

1.2.3 Curcumin

As mentioned before, curcumin is also a good phytochemical that can be found abundantly in turmeric, which is from ginger family.⁷ Curcumin is a bright yellow crystal powder and has bitter taste. Turmeric can be used as a spice in Southeast Asia and India. It has been widely used for thousands of years to treat sprains and swelling caused by injury in those countries. In addition, curcumin has influence on biliary disorders, anorexia, cough, and abdominal pains.²⁶ Curcumin cannot be dissolved in water, but can be dissolved in ethanol and propylene glycol. Recent studies found that curcumin can

inhibit inflammatory reaction. It's a good anti-oxxygenic, anti-rheumatoid, cancer chemopreventive and potentially chemotherapeutic drug.²⁷ Curcumin has been reported to have the ability to suppress the proliferation of many different types of cancer cells, including breast cancer, prostate cancer and colon cancer.²⁸

Previous researches proved that curcumin is very effective in treating breast cancer. It is reported that curcumin causes nutrient deficiency and hypoxia, which will suppress angiogenesis in breast cancer cells and result in cell death.²⁹ Moreover, curcumin has been reported to prevent medroxy progesterone acetate-induced secretion of VEGF from breast T47D cells and this inhibition is dependent on time and dosage.³⁰ Studies showed that the proliferation of breast cancer cell lines, including BT20, SK-BR-3, MCF-7 and T47D is totally blocked by curcumin.³¹ Mehta et al examined the anti-growth effects of curcumin against different types of breast cancer cell lines and demonstrated that curcumin prefers to arrest cells in the G2/S phase. In the meantime, they reported that curcumin can exceed Adriamycin resistance in MCF-7 cells.³² Shao et al presented that curcumin has inhibitive effect on human breast cancer cells in vitro. They used ER (estrogen receptor)-positive MCF-7 cells as well, to do their experiments. The results showed that curcumin prevents the expression of ER genes. Meanwhile, this suppression depends on the presence of estrogen.²⁸

Song et al have studied the effects of curcumin on papillary thyroid cancer cells. They used K1 papillary thyroid cell line to investigate the effects and the potential mechanisms. In their results, curcumin could induce cell non-viability. Meanwhile, cell viability reduced obviously when increasing the concentration of curcumin. Moreover, Song et al demonstrated that the mechanism of curcumin-induced cell non-viability might be due to

the large amount generation of reactive oxygen species (ROS) during the experiment, which resulted in the loss of mitochondrial membrane potential (MMP) as well as the reduction of intracellular Ca^{2+} influx. They summarized that curcumin has low cytotoxic as chemopreventive drug when compared with other chemotherapy drugs.³³

Several studies report the hypothesis that the apoptosis of cancer cells caused by curcumin is because of the p21-mediated cell cycle arrest.³⁴ Watson et al did experiments to make sure whether that hypothesis is correct. They induced curcumin to HCT-116 human colon tumor cells and examined the cell viability through MTT assay. Results showed that curcumin led to apoptosis of HCT-116 cells and this effect was dependent on time and dosage. More importantly, they found curcumin kill both p21^{+/+} and p21^{-/-} HCT-116 cells, which indicated that curcumin-induced apoptosis was not dependent on p21. In addition, they did western blot assay to prove that cell death caused by curcumin was related to a loss of pro-caspase-3 and PARP-1 cleavage.³⁴

1.3 Optoporation

As I mentioned above, many types of phytochemicals and their effects on inhibition of cancer cells, and those phytochemicals are non-toxic. However, those studies mentioned that it would take a long time to see the effects caused by phytochemicals, 12 hours or even more than three days. This is because the plasma membrane of a eukaryotic cell is hardly permeable or even impermeable to most large molecular substances, but it is extremely important to deliver these materials, including most phytochemicals, into tumor cells to reduce their malignant potency.³⁵ Injection of exogenous substances, such as genes, fluorochromes, antibodies and photoactivable compounds into cells is very

necessary for a wide range of applications in many fields including genetics, cell biology, biotechnology and clinical therapy.³⁶ Many techniques have been set up for microinjection of exogenous materials, including chemical methods, electroporation, direct microinjection into cells in a mechanical manner, or through liposome vector.³⁷ However, all these techniques have some dominant disadvantages. For example, these techniques are very strict to the experimental environment and crucial skills, and are usually unsuitable for small animal cells.³⁷ There are also some invasive methods, such as microinjection with microneedles, can be used for single cell injection, but it usually along with a major damage to the cell.³⁸ In consequence, it is essential to find other methods to enable high effective and non-invasive microinjection. This has stimulated exploration of the use of laser-assisted optoporation.

Optoporation is the process of temporarily permeabilizing cells to induce exogenous substance, such as large molecules, into cells by using laser-mediated light. For optoporation, laser beam is usually induced to an absorptive medium on cell membrane, generally polimide or antibody. By interacting with the absorptive medium, optical breakdown, ablation or rapid heating will be produced, which will result in a mechanical transient or gradient photoacoustic wave within the sample. Figure 1.1 can resemble the

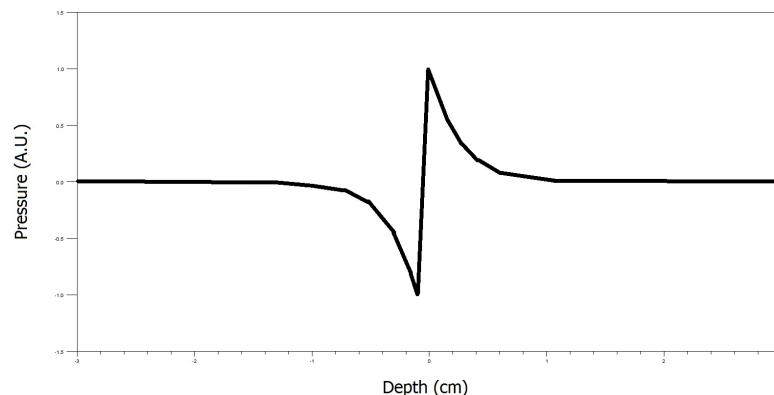


Figure 1.1 The possible photoacoustic wave emitted by sample.

excited photoacoustic wave emitted by sample. This wave generates positive pressure gradient transmits into the liquid. Negative pressure and depth represent acoustic

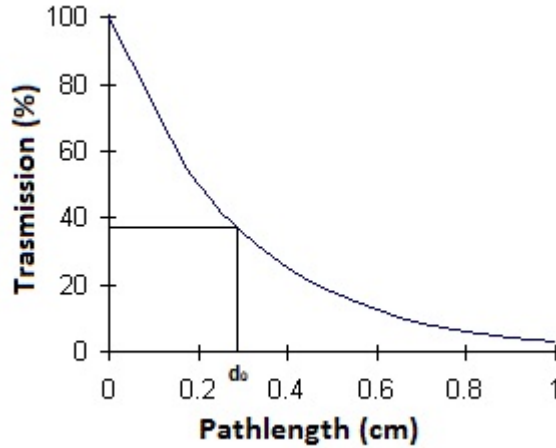


Figure 1.2 Exponential decay of light in the medium as a function of the path length.

reflection at the air-solution interface.³⁹ The pressure decays due to the decline of light transmitted and absorbed by the medium. Figure 1.2 shows the exponential relation between light path length and light transmission. d_0 is the characteristic penetration depth when 37% of the light is travelled while the rest is absorbed. This value has been considered as the characteristic value for experiments.³⁹

When this mechanical photoacoustic wave is not strong enough to damage the cells, it only has temporary effects on cell membranes nearby, including permeabilizing membranes.⁴⁰ There are two important advantages for laser-assisted optoporation. On one hand, this is a contact-free operation and can be used for all types of cells. On the other hand, it can be used either on single cell or more than one cell in suspension, while leaving the cell's architecture intact.³⁸

Nowadays, collimated laser beam has attracted much attention for micromanipulation of single cells because of the high controllability of laser energy as well as the direction

of incident photons, which can be moved by scanning either the beam or sample.⁴¹ Lasers in the UV spectral range, wavelength between 100nm to 400nm, were the first to be studied as the main source of optoporation because of the strong absorption by the components of the membrane in this spectral region. However, the energy of UV light is so strong that can damage the cells. Hence, lasers in the visible region or near infrared are demonstrated more preferred to use. Pulsed visible lasers are usually used for cutting or drilling. Continuous wave lasers are usually used as optical tweezers.³⁷

Samarendra et al used a pulsed nanosecond 1064 nm Nd: YAG laser for microinjection of large impermeable fluorochromes including propidium iodide and merocyanine 540 into MCF-7 cells. The fluorochromes were first suspended in MCF-7 cells culture medium. Then they exposed the edge of each single cell to the 150 μ J per pulse, 17 nanosecond, 10 Hz with energy density around 2.4×10^4 J/cm² laser beam. Timelapse digitized fluorescence video images showed the process of microinjection of fluorochromes into irradiated cells. Also, they found that the fluorochromes uptake was enhanced when laser irradiation time was longer. In addition, they examined the efficiency of nanosecond pulsed laser for transfection. Transfection Cells in the medium with green fluorescent protein encoding plasmid DNA, were irradiated with single pulsed laser of 17-nanosecond duration. After 24 hours laser exposure, they observed green fluorescence in cells, which indicated transfection of gene.³⁷ Optical transfection is a type of Optoporation, and the only difference is that optical transfection is particularly for single cell analysis and usually for delivering nucleic acid, such as DNA, RNA, into cells.

Another method of transferring exogenous materials into living cells was introduced by Yu Zhou et al. They combined the use of liposome microbubble and laser light, as well as ultrasound-microbubble system, for increasing plasma membrane permeability. The theory is similar as talked above, by exposure to laser, they obtained optical breakdown and photoacoustic generation. As they reported, the advantages of liposome microbubble are to increase the cavitation, and meanwhile decrease the damage caused by ultrasound or laser.⁴² In order to choose a kind of laser to blow the liposome microbubbles, they applied different types of laser light and finally decided to use Nd:YAG laser (1064 nm, 4ns). After laser exposure, membrane permeability was tested by flow cytometric assay using propidium iodide (PI) and fluorescein diacetate (FDA). As expected, the extracellular membrane-impermeable molecules could be delivered into living cells by the combination laser-microbubble system. At the same time, this result was affected by the energy of laser.⁴²

There are also many studies using femtosecond lasers as the light source for optical transfection because of its precise property. The mechanism for femtosecond laser is different with others. Femtosecond laser makes cell membrane permeable temporarily through multiphoton process and the damage caused by femtosecond laser irradiation is well below the threshold due to these multiphoton mechanisms are mostly localized in the femtosecond regime. However, femtosecond laser has low efficiency that needed to be improved urgently.⁴³ Femtosecond (fs) laser used to be applied for the transfection of human hepatocarcinoma (HepG2) cells at the wavelength of 1554 nm with other parameters of 20 MHz, 170 fs and energy density around 10^{12} W/cm². The results showed

that HepG2 cells could be permeable to propidium iodide in a short time. In addition, no mitochondrial depolarization was observed.⁴⁴

Instead of directly inducing laser to cell membrane, many researches use nanoparticles to absorb light energy, which is more efficient than physical laser irradiation. Small particles like nanoparticles have great optical absorption from laser exposure. Previous research demonstrated that carbon nanoparticles generated high temperature after short time of laser irradiation.⁴⁵ Aside from the chemical reaction, the acoustic waves were agenerated due to the transient changes in the density and pressure fields of the surrounding caused by extremely rapid irradiation.⁴⁶ Chakravarty et al did experiments using femtosecond laser pulses to activate carbon black (CB) nanoparticles, which enabled the delivery of large molecules, such as proteins and DNA, into cells.⁴⁷ To test the delivery efficiency of laser activation of CB, Chakravarty et al conjugated CB nanoparticles to human DU145 prostate cancer cells and then mixed the suspension with calcein, bovine serum albumin (BSA) of plasmid DNA encoding luciferase expression. 800 nm femtosecond laser pulses were induced to the suspension with laser energy that can overcome the threshold of photoacoustic activity. Results showed that more than 90% of DU145 prostate cancer cells contained calcein and over 35% contained BSA. For fluorescently encoded DNA, they also observed about 22% of cells revealed encoded DNA positive. Results also suggested that the uptake of these materials was affected by the laser energy and exposure time.⁴⁷ Generally speaking, Chakravarty et al demonstrated that photoacoustic forces were generated by the interaction between the laser energy and CB nanoparticles and transient openings in the membrane for intracellular delivery were created by chemical reaction.⁴⁷

Methods using laser-absorbing gold nanoparticles-coated substrate have been attracted much interest recently. Gold nanoparticles have different size and shape properties with bulk gold. They have a high surface area to volume ratio and can be modified with different types of functional ligands.⁴⁸ Gold nanoparticles can absorb electromagnetic radiation strongly near their plasma resonant frequency. Their advantages including response fast, relatively stable and easy to deal with make them widely used in the thermoplasomics field.⁴⁹ Gold nanoparticles can generate heat under illumination. These light-absorbing nanoparticles are generally bound to cell membranes by means of immunochemistry, including amine, peptide, antibody and lipid ligands,⁴⁸ and then exposed to lasers. The purpose is to localize all the laser-absorptive effects only to the gold nanoparticles-targeted cell membranes. Laser irradiation wavelength, pulse duration and the ability of the absorbing nanoparticle structure affect the cell treatment. Yao et al used this technique with different laser sources and different pulse durations, to deliver exogenous molecules into human lymphoma cell lines L-428 and Karpas-299, similar to the work of Chakravarty et al.⁵⁰ Their results showed that for single pulse irradiation mode, cell permeable ability decreased and cell non-viability increased when the number of pulse larger than the optimal five pulses. On the other hand, for scanning mode, further more number of pulses had no obvious effects on cell permeability and cell death.⁵⁰ However, they chose gold nanoparticles with the diameter of 30 nm and 15 nm, which can be optimized to the laser irradiation wavelength of 532 nm. A 50 nm gold nanoparticle has a three- to four-fold higher efficiency of absorption at a 532 nm wavelength.⁵¹

Overall, the main issue is to increase the cell membrane permeability to introduce exogenous macromolecules, such as phytochemicals, into the cancer cells. Currently, a method that can selectively increase the permeability of desired cells with conjugated gold nanoparticles and localize the damage to the targeted cell membrane needs to be studied. Bhattacharyya et al demonstrated that they bound antibody-conjugated gold nanoparticles to breast cancer cell membranes by immunochemistry method. Their irradiation parameters in the experiments were Q-switched 5 nanosecond pulses with a wavelength of 532 nm laser. They irradiated the gold nanoparticle-bound cells with different radiant exposures of 10 to 40 mJ/cm² for up to 800 pulses. Cell membrane permeability was increased through this optical absorption. As reported, they indicated that for 20 and 40 mJ/cm² irradiation, up to 70% cells became permeable at 800 pulses. At the same time, relatively lower cell non-viable were caused by 20 mJ/cm² when compared to 40 mJ/cm².⁵²

In order to change the permeability of the breast cancer cells, this study used the same Q-switched 532 nm laser and according to Bhattacharyya et al, radiant exposure of 20 mJ/cm² was used to irradiate the targeted cells bound with gold nanoparticles. We applied gold nanoparticles here because of their peak absorption near the harmonic laser wavelength of 532 nm. Phytochemicals were more easily transferred into cells right after increasing permeability by gold nanoparticle-coated laser irradiation. On the other hand, those non-irradiated cells kept impermeable to.

Chapter 2

Materials and Methods

2.1 Materials

2.1.1 Cell Culture

T47D cell lines from human breast cancer tissue were obtained from Cell and Immunology Core (CIC) at the University of Missouri-Columbia. Those cells were cultured in 2.5 mL DMEM growth medium in 35 mm diameter as well as optically clear petri dish with a concentration of about 10^6 cells/mL and incubated at a 37°C, 5% CO₂ incubator. T47D cells were confluent and they covered on the base of the petri dish completely before using them. In addition, T47D cell line is naturally colorless, so intracellular heating did not happen to affect the experiments.

2.1.2 Reagents

Spherical gold nanoparticles (Au NPs) 54 nm in diameter functionalized with neutravidin were bought from Nanopartz Inc at a concentration of 5×10^{12} nanoparticles/mL; 3×10^{15} molecules/mL anti-epithelial cell adhesion (anti-EpCAM) functionalized with biotin was bought from Pierce Antibody; calcofluor white M2R (MW: 960.9 g/mole) was obtained from Sigma-Aldrich co; trypan blue was purchased from Sigma-Aldrich co; polyethylene glycol 200 and 400(PEG200 and PEG400) was from Thermo Fisher Scientific Inc; β -carotene was purchased Fluka Analytical; dipalmitoyl-sn-glycero-3-phosphocholine (DPPC) was bought from Sigma-Aldrich co.

2.1.3 Equipment

The Nd: YAG Q-switched laser with a 5 ns pulse was bought from Continuum; the microscope we used is an inverted IX70 Olympus widefield microscope with fluorescent lamp from Molecular Cytology Core (MCC) at Life Sciences, University of Missouri-Columbia. System control and image acquisition were done with MetaMorph software.

2.2 Experimental Methods

2.2.1 Pretreatment Procedure of Conjugation of Au NPs and T47D Breast Cancer Cells

As mentioned before, Au NPs have already functionalized with neutravidin, anti-EpCAM has already functionalized with biotin. Neutravidin protein is a deglycosylated product from avidin. It is still like avidin that processes strong biotin-affinity characteristics due to the molecular structural complementation. Additionally, because of its near-neutral pI, neutravidin hardly interacts with the negatively charged cell surface.⁵³ In this way, Au NPs conjugated with neutravidin and anti-EpCAM conjugated with biotin can be bound together. On the other hand, NPs can be attached to cancer cells by functionalizing the NPs with antibody, such like anti-EpCAM. As a membrane glycoprotein, EpCAM is highly expressed on most cancer cells, and in breast cancer, high expression of EpCAM was observed before.⁵⁴ Therefore, Au NPs can be conjugated to breast cancer cell membrane due to the conjugation of cell surface EpCAM antigen and Au NPs coated antibody anti-EpCAM. Figure 2.1 explains the principle of the attachment of Au NPs and T47D breast cancer cells.

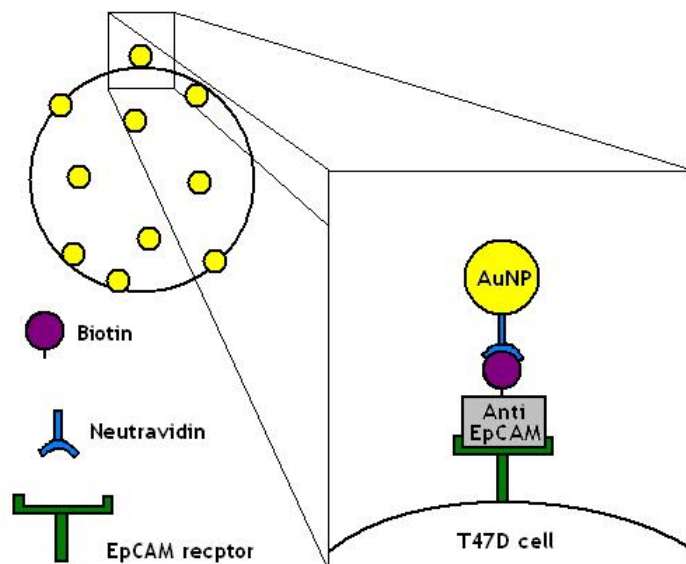


Figure 2.1 This figure shows the principle conjugation of Au NPs and T47D cells. Biotinylated anti-EpCAM was bound to Au NPs first, then EpCAM receptors on cell membrane recognized and combined anti-EpCAM with Au NPs. Note that figure is not to scale.

Mix up neutravidinlyated Au NPs and biotinylated anti-EpCAM. According to Bhattacharyya et al, about five to ten anti-EpCAM antibodies fit one Au NP. Before the cell treatment, we observed the coverage of cells under the microscope to make sure that the cells were covering well. First added 2 μL of anti-EpCAM antibody into 1 mL 1 \times PBS in tube. Then 50 μL of the stock solution was added into the anti-EpCAM solution. Mixed the solution by vibrator and then wait for about 30 to 45 min allowing reaction of Au NPs and anti-EpCAM. Centrifuged the mixed solution of Au NPs and anti-EpCAM at 8000 rpm for 8 min. The supernatant along with unbound anti-EpCAM antibody was removed, leaving anti-EpCAM conjugated Au NPs resuspended in 1 mL of 1 \times PBS. After, this solution was stock in the refrigerator for less then two weeks and ready to be used.

200 μL of the stock solution of antibody conjugated Au NPs was added into cell dish and incubated for 1 h. Those values of analytes were obtained by plenty of tests as well as previous work.⁵²

2.2.2 Optoporation

After incubation of 1 h for Au NPs conjugating to cell membrane, growth medium was taken out and unbound Au NPs were cleaned by 1 mL of $1\times$ PBS washing. Then 1mL of treatment solution including phytochemicals or $1\times$ PBS was added into the cell dish and then the cell dish was ready to be irradiated with the laser. Q-switched laser with 20 Hz and 5 ns pulses at the wavelength of 532 nm was used to irradiate the sample. Based on work of Bhattacharyya et al, 400 pulses and $20 \text{ mJ}/\text{cm}^2$ were applied in this study due to the large cell permeabilization and low cell death caused by this condition.⁵² 400 pulses equals to 20 s of exposure. We used 0.134 cm^2 of area for each circle in this study. Pulsed laser was adjusted by a converging lens with a 150 mm focus and delivered by a 1mm optical fiber as seen in figure 2.2. Before exposing to the cell dish, the optical fiber needed to be aligned to make sure it was vertical to the dish. Additionally, fiber was collimated up and down to make sure the area was 0.134 cm^2 . After aligning the fiber, pulse energy was measured and adjusted to around 2.68 mJ by using energy meter. After modulating the energy, five spots were irradiated in one cell dish as shown in figure 2.2.

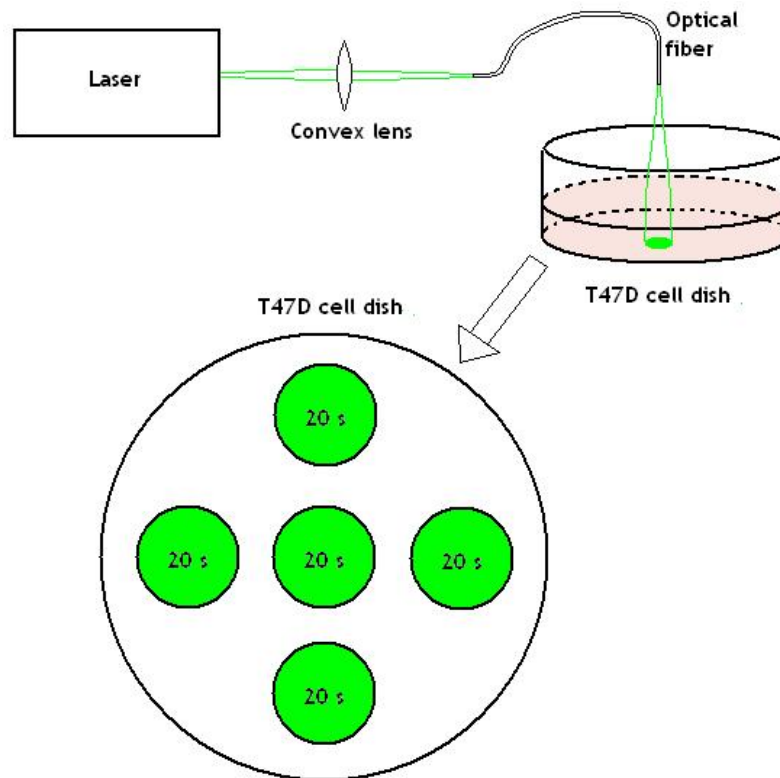


Figure 2.2 Laser was adjusted by a convex lens and guided by optical fiber to the cell dish with treatment solution. Five spots were irradiated in the cell dish and 20 s for one spot. Note that figure is not to scale.

Two to three cell dishes were treated each time with the same condition for more sets of data.

2.2.3 Fluorescent Test

Previous work has done to confirm the theory of Bhattacharyya et al by fluorescent test. Calcofluor white M2R was used to confirm since this fluorescent agent is too large to get into a normal breast cancer cell. Calcofluor white M2R was dissolved in $1\times$ PBS at the concentration of $250\ \mu\text{g}/\text{mL}$ and stocked avoiding light. After the pretreatment step, 1 mL $1\times$ PBS was added into cell dish and exposed to laser. Then Calcofluor white M2R

was added into cell dish along the dish wall carefully since the cell membranes were opened already. 30 min later, cell membranes were closed again and the fluorescent dye solution was taken out. Cells were washed by 1× PBS to remove the excessive fluorophor and resuspended in 1 mL of 1× PBS. Imaged sample under IX 70 Olympus fluorescence microscope and the percentage of permeable cells were measured by using imageJ. We will explain the use of imageJ in Appendix A.

We took the pictures from borders and centers of the five irradiated area. Figure 2.3 shows the result of fluorescent test. We can see that in the irradiated area, most cells were bright because fluorescent dye went into cells after exposure to laser. The rest non-irradiated area was almost black, only few white dead cells. Cell death in the irradiated area was measure by imageJ with a value of 92.7%. On the other hand, Bhattacharyya et al reported that the nonviable cell percentage of exposure of 20 mJ/cm² with 400 pulses was less than 5% and cell permeability at the same condition was 50% determined by

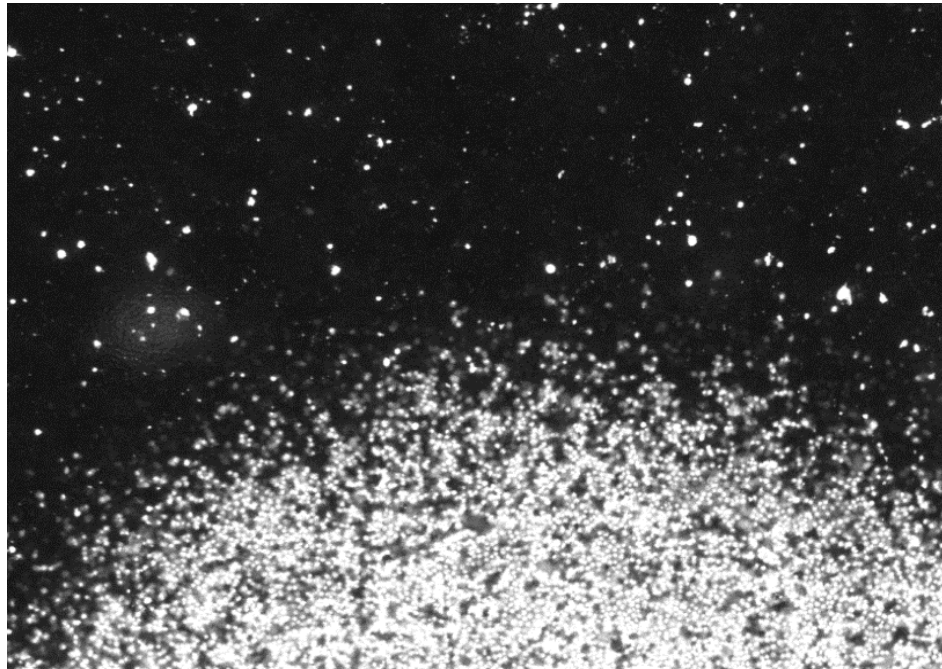


Figure 2.3 Border of the irradiated spot. White dots are fluorescent cells.

fluorescence. However, Calcufluor white M2R can also stain dead cells,⁵⁵ therefore, the values of cell permeability should be smaller than what they got. But actual cell permeability is still high even after minus 5% nonviable cells at the condition of 20 mJ/cm² irradiation with 400 pulses. This high cell death confirmed the theory that optoporation is an effective method to enhance cell permeabilization.

2.2.4 β -Carotene/PEG Test

β -Carotene is hardly soluble in water but easy soluble in benzene, chloroform, etc, which are usually toxic to cells. Therefore, it is important to find a method to dissolve β -carotene. Here, we tried PEG200, PEG400 and DPPC liposomes to dissolve β -carotene.

PEG is a polyether compound that has been widely used in industrial and medical manufacturing. PEGs are made of polymerized ethylene oxide and there are many forms base on a wide range of molecular weights from 200 g/mol to 20000 g/mol. PEG is intermiscible with water and many other organic solvent hence it has been used by researchers to dissolve β -carotene at the concentration from 0.1 to 1 mg/mL.⁵⁶

3%, 5%, 7%, 10%, 15%, 20% (volume rate) of PEG200 and PEG400 were made in 1 \times PBS and mixed well. After pretreatment of cells, growth medium with excessive Au NPs were removed and 1 mL of stocked PEG solution was added into cell dish. Then cell dish with PEG solution was irradiated with laser. Kept on incubating for 30 min after laser treatment and then removed PEG solution. Cells that still have activity would recover during the 30 min incubation, while dead cells wouldn't. Hence, 1 mL of 250 μ g/mL Calcoflur white M2R fluorescent dye solution was used to see if cell membrane was

completely destroyed after laser treatment due to the large molecular fluorescent dye can only stain dead cells.⁵⁵ Fluorescent dye solution was removed after another 30 min, and cell dish cleaned by 1× PBS carefully in order to clean out excessive fluorophor. Then resuspended with 1 mL of 1× PBS, images were taken by IX 70 Olympus fluorescent microscope. Cell death was measured by imageJ.

On the other hand, β -carotene/PEG solution was obtained by dissolving in pure PEG at the concentration of 1 mg/mL and then the mixed solution was diluted respectively to 3%, 7%, 15% and 20% in volume ratio (PEG: 1× PBS). After pretreatment of cells with Au NPs, cell dish with 1 mL of β -carotene/PEG solution was exposed to laser. Incubated for 30 min, took out β -carotene/PEG solution, 1 mL of fluorescent dye solution was added for 30 min. Then sample was washed by 1× PBS carefully and resuspended in 1 mL of 1× PBS. Sample was imaged by IX 70 Olympus fluorescent microscope and cell death was measured by imageJ.

2.2.5 Control group test

2.2.5.1 Absorption of Laser Treatment Solutions

Absorptions of laser treatment solutions were examined by spectrophotometer from NanoDrop co. The solutions include Au NPs solution, PEG200, PEG400, PEG200 in the presence of β -carotene, PEG400 in the presence of β -carotene, Au NPs solution with PEG200 in the presence of β -carotene and Au NPs solution with PEG400 in the presence of β -carotene. Note that the Au NPs solution was the solution that has been conjugated with anti-EpCAM and PEG solutions were pure for absorption test. Additionally the concentration of β -carotene was 1 mg/mL in PEG solution.

2.2.5.2 Cells with Membrane-bound Au NPs and Incubate with PBS

After pretreating cells, Au NPs have conjugated to cell membrane. 1 mL of 1× PBS was added into cell dish. Exposure of laser with 20 sec was applied for each circle area in the cell dish. Cell dish was incubated 30 min for cell membrane's recovery. Then fluorescent dye solution was added into cell dish for another 30 min. Fluorescent dye solution was cleaned by washing with 1× PBS carefully, then suspended in 1 mL of 1× PBS. Control sample was imaged by fluorescent microscope. Cell death was measured by imageJ.

2.2.5.3 Cells without Membrane-bound Au NPs and Incubate with PEG200 and PEG400

We also did experiment to see if PEG200 and PEG400 affect cell proliferation when irradiating the cells without Au NPs. Cell growth medium was removed and resuspended in 1 mL of 20% PEG200 or 20% PEG400 respectively. Exposure of laser with 20 sec of 20 mJ/cm² energy and then took out PEG200 after incubating 30 min. Fluorescent dye solution was added into the cell dish for 30 min, washed away with 1× PBS carefully and resuspended in 1 mL of 1× PBS. Sample was imaged under IX70 Olympus microscope and cell death was measured by imageJ.

2.2.6 β-Carotene/DPPC Liposomes Test

Two delivery methods of β-carotene were studied by many researchers, include solubilizing in the organic solvent tetrahydrofuran (THF) and DPPC liposomes. However, THF affects cell proliferation and induces cell death. In contrast to THF, DPPC liposomes doesn't have influence on cell activity.⁵⁷

Here, we chose DPPC liposomes method to dissolve β -carotene. β -Carotene was soluble in chloroform at the concentration of 2.68 mg/mL. 20 mg of DPPC powder was dissolved in 500 μ L of chloroform in the presence of β -carotene. The lipid solution was dried with nitrogen, then resuspended in 10 mL of 1 \times PBS and unilamellar vesicles were generated by 15 min sonication.⁵⁷ After cell pretreatment, 1 mL of β -carotene/DPPC solution was added into cell dish and irradiated with 20 mJ/cm² energy. Then similar to previous work, 1 mL of fluorescent dye solution was used to stain living cells for 30 min. Sample was washed by 1 \times PBS and then imaged by fluorescent microscope and cell death was measured by imageJ.

2.2.7 Tetracycline Test

We also used tetracycline as the drug to kill the T47D cells since tetracycline has been widely used as anti-biotics in many areas, including melanoma, breast cancers. Tetracycline is isolated from the streptomycetes genus of actinobacteria with the property of inhibiting protein synthesis. During the inhibition process, tetracyclines bind to the 30S subunit of microbial ribosomes and then block the attachment of charged aminoacyl-tRNA to the A site on the ribosome. In this way, they block the introduction of new amino acids to the nascent peptide chain.⁵⁸

In this study, we made 1 mg/mL of tetracycline in 1 \times PBS. After pretreatment, tetracycline was added in the cell culture dish and irradiated by laser for 20 seconds each time. Then incubated 1 mL of DMEM and put in the incubator for 2 hours. After, solutions were absorbed out and 1 mL of trypan blue was added into cell dish for 5 min. Images were taken after cleaning out trypan blue.

Chapter 3

Result

3.1 Cell Death Caused by PEG Solutions in the Absence of β -Carotene

Fluorescence image show the increasing cell permeability of irradiated regions cells caused by (a) 3% PEG200, (b) 5% PEG200, (c) 7% PEG200, (d) 10% PEG200, (e) 15% PEG200 and (f) 20% PEG200 in the absence of β -carotene as seen in figure 3.1. The blue dots indicate dead cells since nonviable cell membranes have been destroyed and fluorophor could attached dead cells, while dark regions indicate living cells that have recovered to healthy membranes during the 30 min incubation, hence large molecular Calcofluor white M2R couldn't diffuse into the cells. Fluorescent solution was cleaned

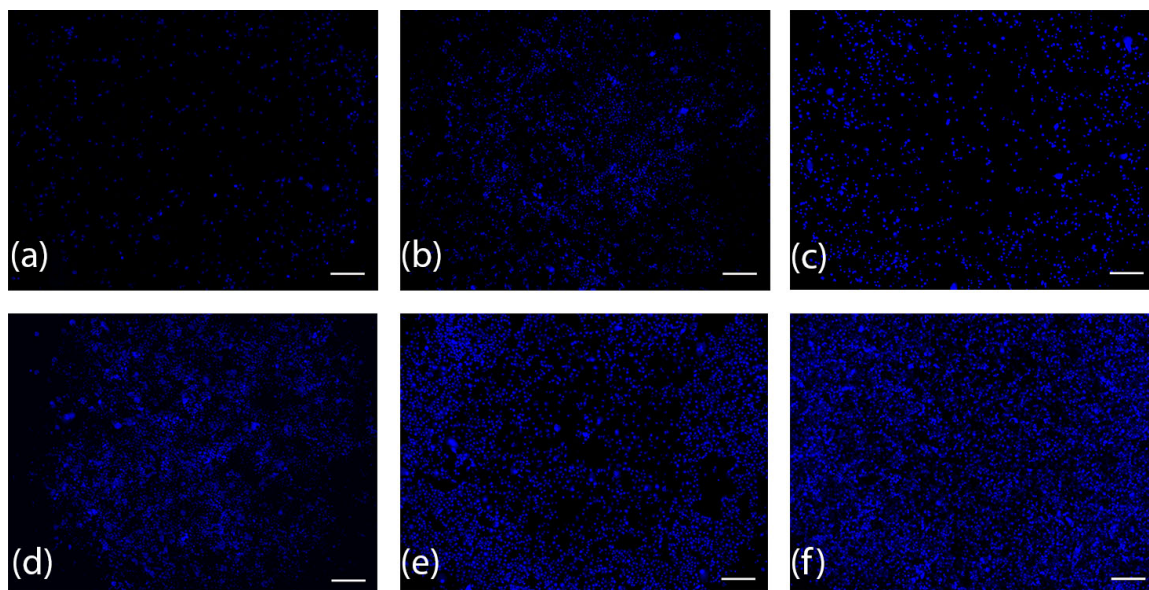


Figure 3.1 (Color online) Fluorescence images of increasing cell permeability from (a) 3% PEG200, (b) 5% PEG200, (c) 7% PEG200, (d) 10% PEG200, (e) 15% PEG200, (f) 20% PEG200 in irradiated regions of the cell culture dish. The blue dots indicate dead cells. Scale bar is 200 μ m.

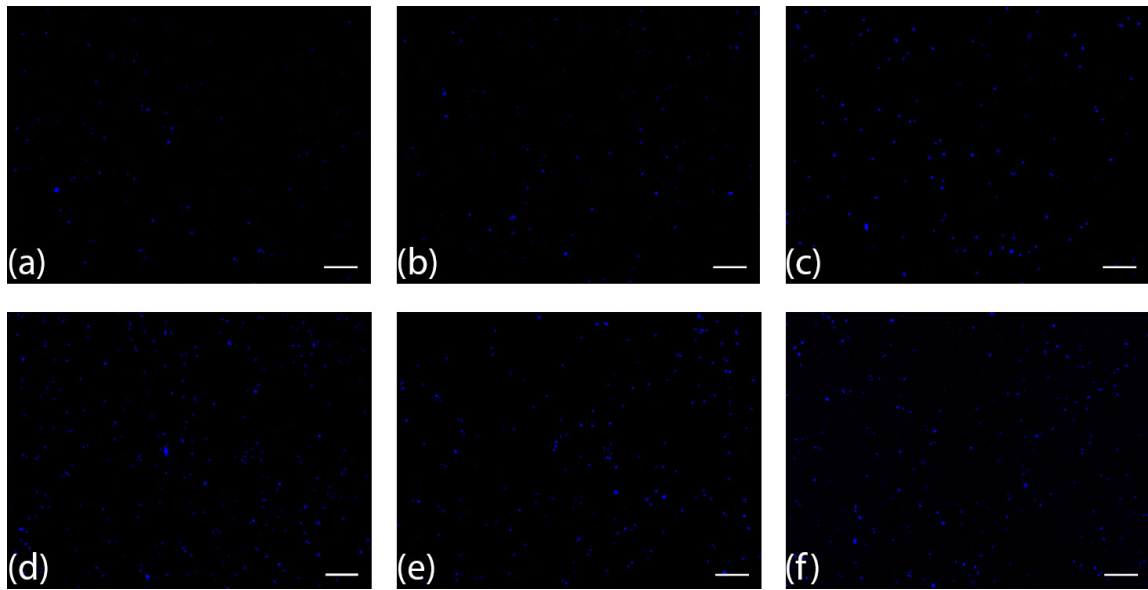


Figure 3.2 (Color online) Fluorescence images of non-irradiated cell permeability from (a) 3% PEG200, (b) 5% PEG200, (c) 7% PEG200, (d) 10% PEG200, (e) 15% PEG200, (f) 20% PEG200 in non-irradiated regions of the cell culture dish. The blue dots indicate dead cells. Scale bar is 200 μm .

by 1 mL of $1\times$ PBS before imaging. As indicated in figure 3.1, more blue fluorescence can be seen when increasing the concentration of PEG 200. In addition, non-irradiated regions of different concentrations of PEG200 were also imaged to measure the non-irradiated cell death as shown in figure 3.2. Five non-irradiated spots were also chosen to expose to laser with the same energy and pulses. Images show few blue dots, which indicate that cell death in non-irradiated regions is not high.

Table 3.1 lists the cell death caused by different concentrations of PEG200, with the average value of 3.38% for 3% PEG200, 6.02% for 5% PEG200, 10.97% for 7% PEG200, 13.93% for 10% PEG200, 16.51% for 15% PEG200, 23.63% for 20% PEG200. Figure 3.3 shows rising trend with standard deviation. It demonstrates that cell death is increased when enhancing the concentration of PEG200, which indicates that higher concentration of PEG200, higher cell death can be obtained. ANOVA test ($\alpha=0.05$) on the cell death shows $p<0.05$, which means there is significantly more cell death when

increasing the concentration of PEG200, even though when compared 10% PEG200 and 15% PEG200, $p>0.05$. Additionally, as shown in table 3.1, cell death from non-irradiated area was also measured by imageJ, with the average value of 1.09% for 3% PEG200, 0.72% for 5% PEG200, 0.75% for 7% PEG200, 1.28% for 10% PEG200, 0.95% for 15% PEG200, and 0.78% for 20% PEG200. Those values indicate the similar cell death from non-irradiated regions.

Table 3.1 Irradiated and non-irradiated cell death caused by different concentrations of PEG200

Concentration of PEG200	Irradiated cell death	Non-irradiated cell death
3%	3.38%	1.09%
5%	6.02%	0.72%
7%	10.97%	0.75%
10%	13.93%	1.28%
15%	16.51%	0.95%
20%	23.63%	0.78%

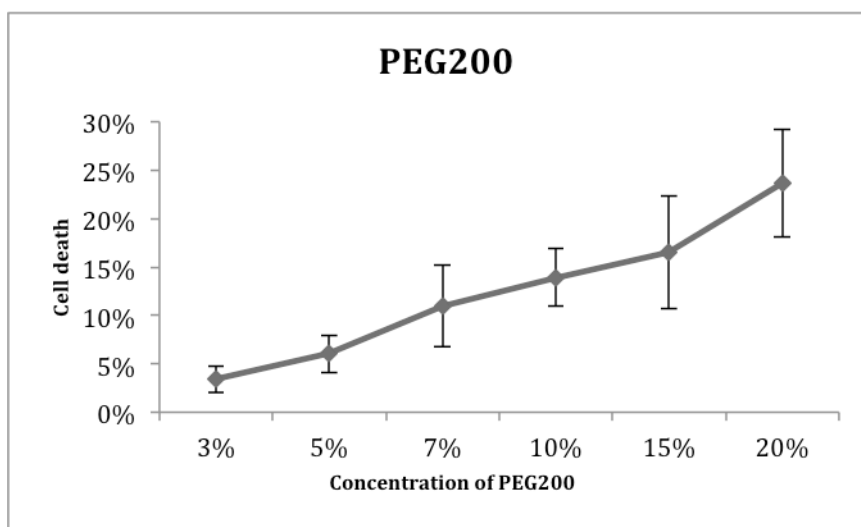


Figure 3.3 Percent of non-viable cells with Au NPs suspended in different concentration of PEG200. The results show a rising cell death when increasing the concentration of PEG200.

Fluorescence pictures of PEG400 were also imaged as shown in figure 3.4, which also shows the slightly increasing amount of dead cells of irradiated regions from (a) 3% PEG400, (b) 7% PEG400, (c) 15% PEG400 and (d) 20% PEG400, although the cell

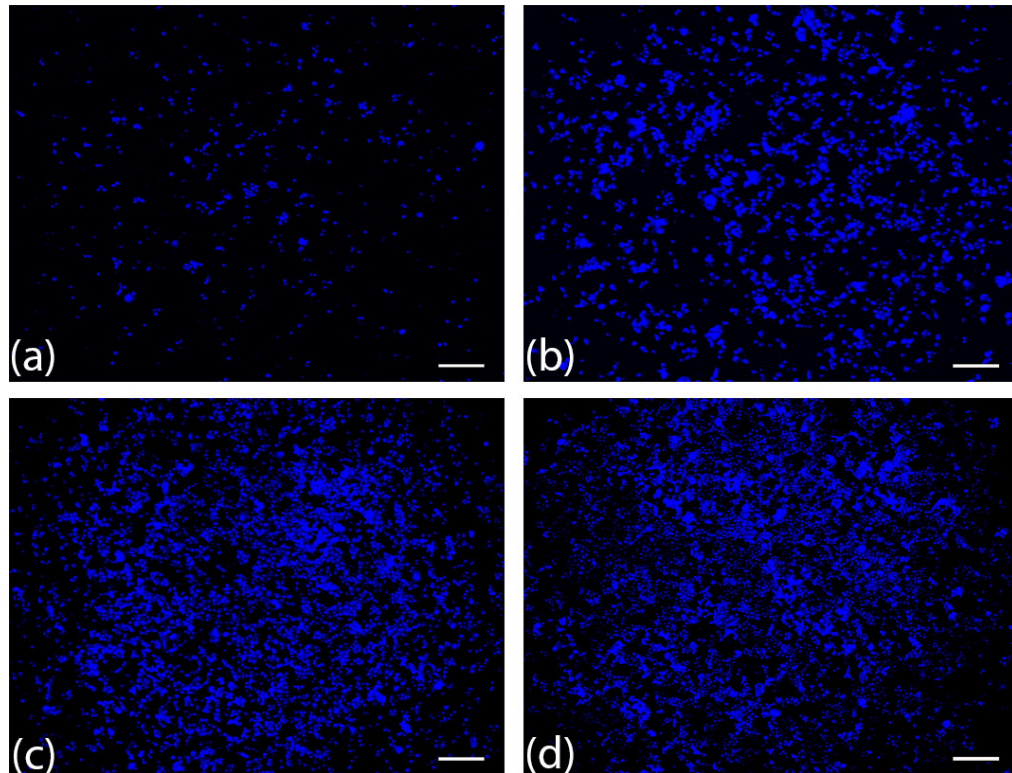


Figure 3.4 (Color online) Fluorescence images of increasing cell permeability from (a) 3% PEG400, (b) 7% PEG400, (c) 15% PEG400, (d) 20% PEG400 in irradiated regions of the cell culture dish. The blue dots indicate dead cells. Scale bar is 200 μm .

permeability from figure 3.3 (c) and figure 3.3 (d) look similar. Non-irradiated regions of cells suspended in PEG400 were also imaged and cell death was measured by imageJ, and the images are similar to those as seen in figure 3.2.

Similarly, table 3.2 lists the average cell death of each concentration of PEG400 and figure 3.5 shows the rising cell death of 5% PEG400, 7% PEG400, 15% PEG400 with standard deviation. ANOVA test ($\alpha=0.05$) also proved that there is significantly more cell death when increasing the concentration of PEG400. This phenomenon also indicates that when suspended in higher concentration of PEG400, more cells can be killed under the same condition of laser treatment. On the other hand, non-irradiated cell death kept similar and cell non-viability is low when compared to irradiated area.

Table 3.2 Irradiated and non-irradiated cell death caused by different concentrations of PEG400

Concentration of PEG400	Irradiated cell death	Non-irradiated cell death
3%	2.31%	0.28%
7%	9.50%	0.28%
15%	18.85%	0.37%
20%	20.67%	0.29%

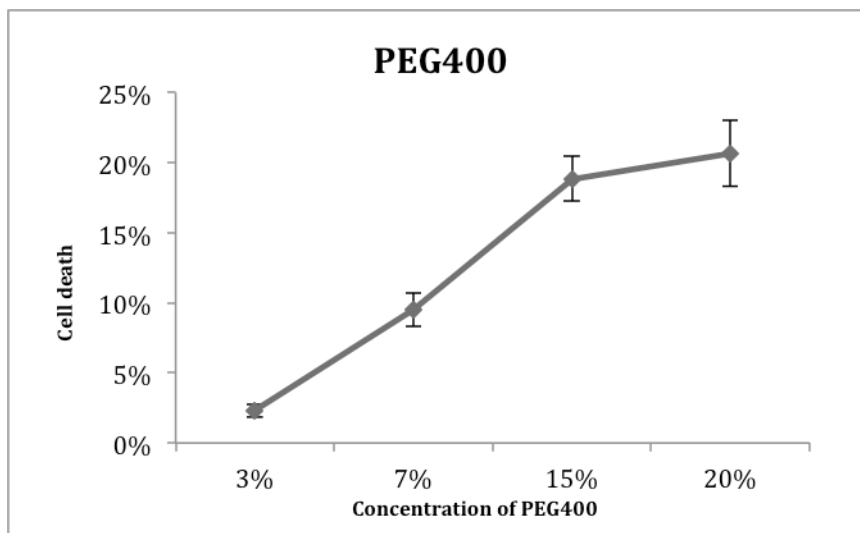


Figure 3.5 Percent of non-viable cells with Au NPs suspended in different concentration of PEG400. The results show a rising cell death when increasing the concentration of PEG400.

3.2 Cell Death Caused by PEG Solutions in the Presence of β -Carotene

β -Carotene was added into pure PEG200 and PEG400 at the concentration of 1 mg/mL. Then β -carotene/PEG solutions were diluted to 3%, 5%, 7% and 15% in $1 \times$ PBS as discussed above. Images of cells treatment by β -carotene/PEG were collected as seen in figure 3.6, which shows the fluorescent cell death of different concentrations of PEG 200 in the presence of β -carotene. We can also tell obviously that blue fluorescence is stronger in figure 3.6 (c) and figure 3.6 (d) than in figure 3.6 (a) and figure 3.6 (d), which indicate that cell permeability is increased when increasing the concentration of both β -

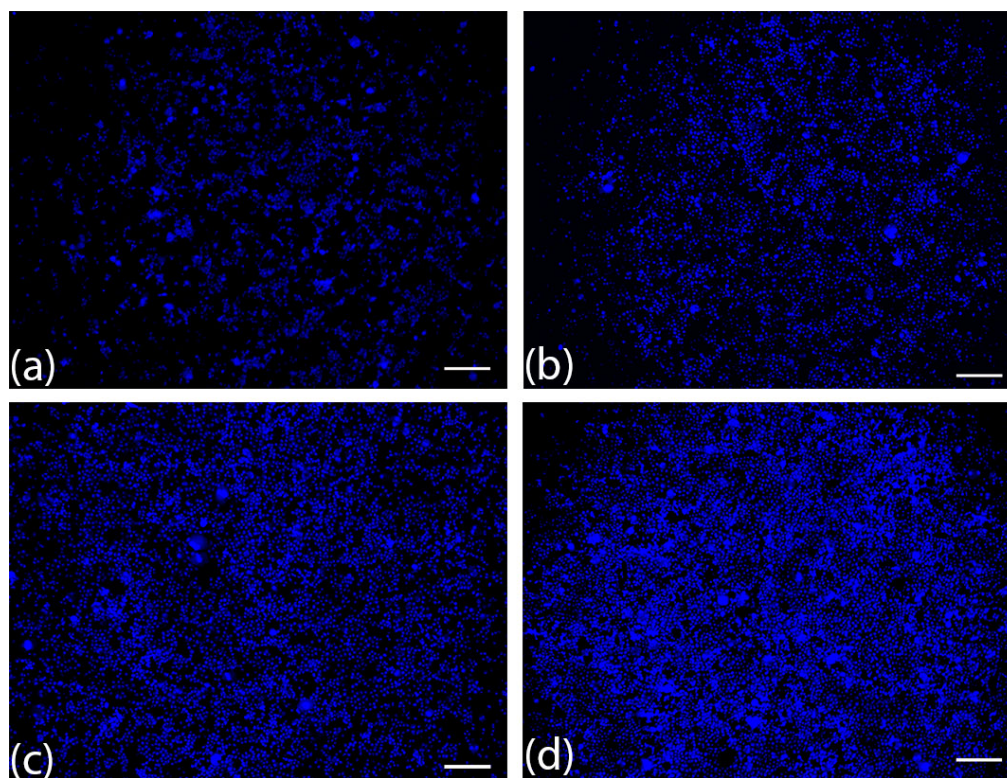


Figure 3.6 (Color online) Fluorescence images of increasing cell permeability from (a) 3% β -carotene/PEG200, (b) 7% β -carotene/PEG200, (c) 15% β -carotene/PEG200, (d) 20% β -carotene/PEG200 in irradiated regions of the cell culture dish. The blue dots indicate dead cells. Scale bar is 200 μ m.

carotene and PEG200. Figure 3.7 also indicates the increasing cell death for the concentrations of β -carotene/PEG200 solutions from 3% to 20%. ANOVA test ($\alpha=0.05$) demonstrates that there is obviously increasing cell death when the concentration of β -carotene/PEG200 is larger. Same phenomenon can also be seen in figure 3.8 and figure 3.9 of increasing concentration of PEG400 in the presence of β -carotene. ANOVA test ($\alpha=0.05$) also proves the obviously increasing cell death as the concentration of β -carotene/PEG400 larger. Additionally, table 3.3 and table 3.4 show both irradiated and non-irradiated cell death resulted from PEG solutions in the presence of β -carotene.

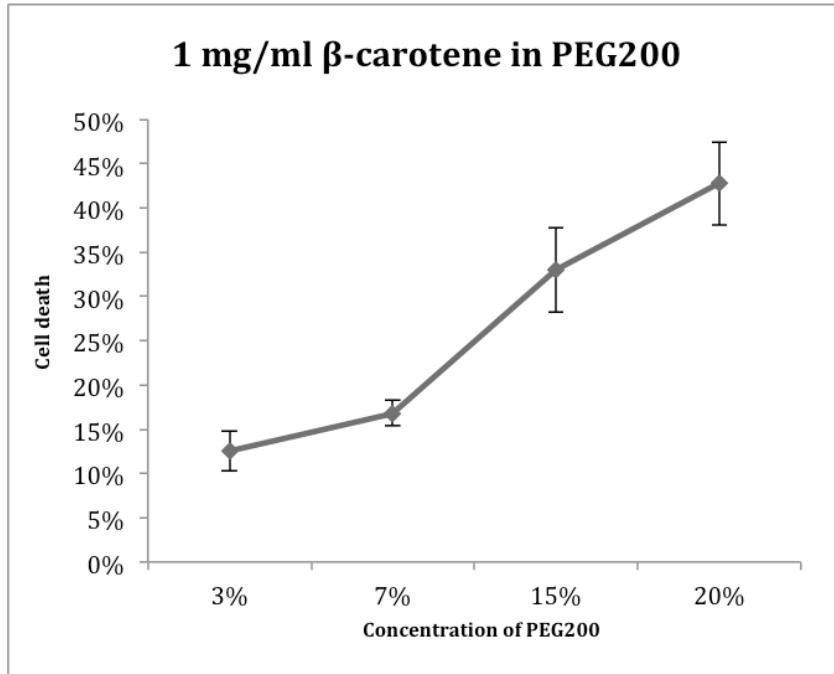


Figure 3.7 Percent of non-viable cells with Au NPs suspended in different concentration of β -carotene/PEG200. The results show a rising cell death when increasing the concentration of β -carotene/PEG200.

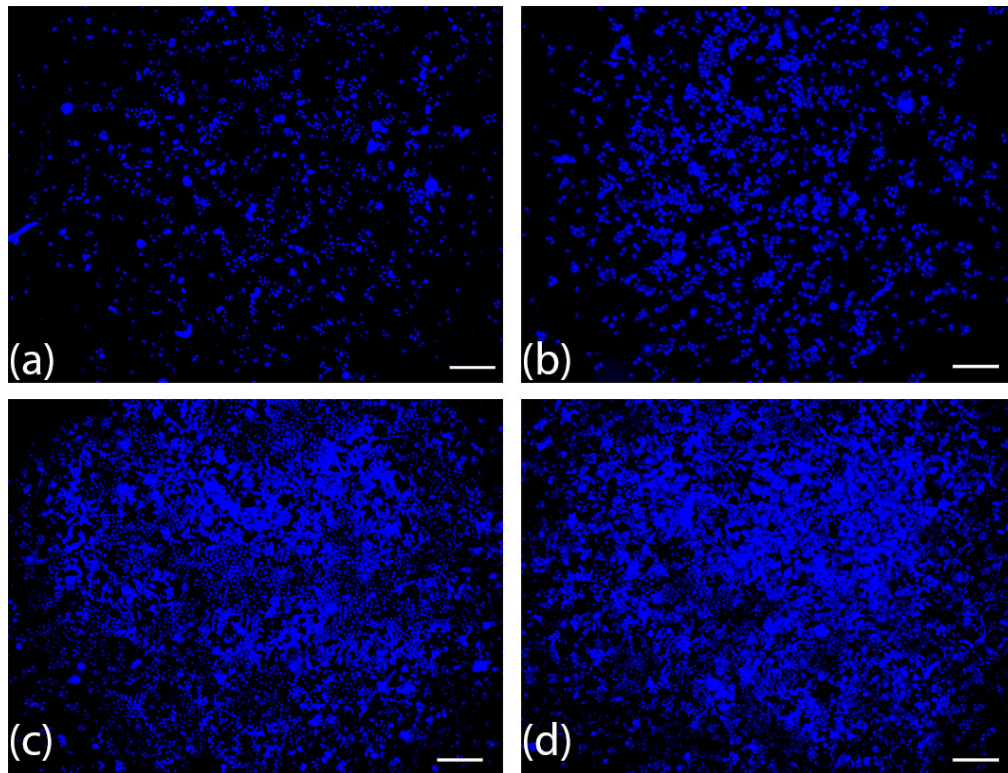


Figure 3.8 (Color online) Fluorescence images of increasing cell permeability from (a) 3% β -carotene/PEG400, (b) 7% β -carotene/PEG400, (c) 15% β -carotene/PEG400, (d) 20% β -carotene/PEG400 in irradiated regions of the cell culture dish. The blue dots indicate dead cells. Scale bar is 200 μ m.

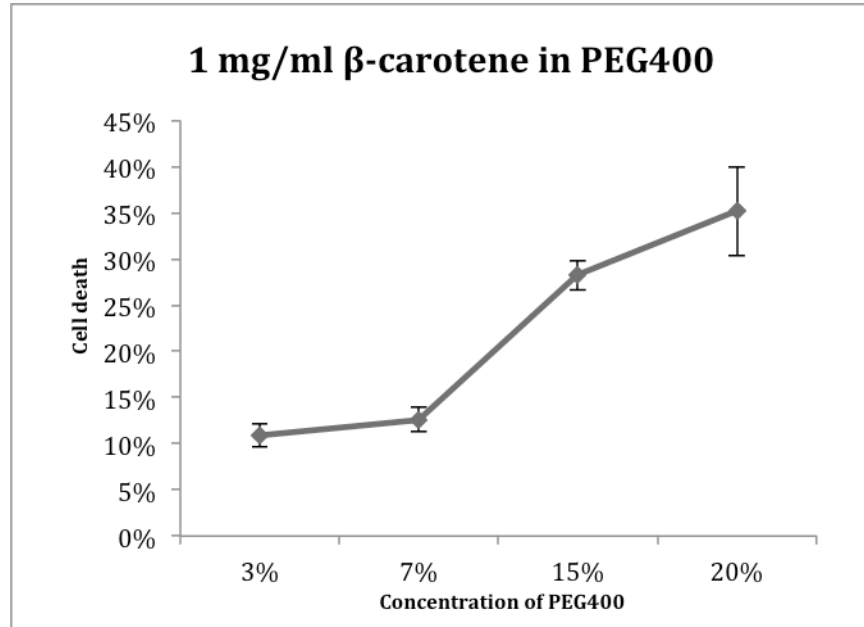


Figure 3.9 Percent of non-viable cells with Au NPs suspended in different concentration of β -carotene/PEG400. The results show a rising cell death when increasing the concentration of β -carotene/PEG400.

Table 3.3 Irradiated and non-irradiated cell death caused by different concentrations of β -carotene/ PEG200 solution

Concentration of β -carotene/PEG200	Irradiated cell death	Non-irradiated cell death
3%	12.53%	1.02%
7%	16.82%	0.33%
15%	32.99%	1.29%
20%	42.79%	1.19%

Table 3.4 Irradiated and non-irradiated cell death caused by different concentrations of β -carotene/ PEG400 solution

Concentration of β -carotene/PEG400	Irradiated cell death	Non-irradiated cell death
3%	10.88%	0.27%
7%	12.63%	0.27%
15%	28.21%	0.21%
20%	35.15%	0.32%

3.3 Results of Control Groups

3.3.1 Confirmation of Light Absorbance of Treatment Solutions

As discussed above, we also did some control experiments. First, we measured the absorbance of all materials that cells were suspended in and treated with laser exposure to make sure they don't absorb light when heating with laser, only Au NPs can absorb light and figure 3.10 can prove this. Since the wavelength we used in the experiments was 532 nm, we can just focus on the absorbance at the wavelength at 532 nm. From figure 3.10 we can observe that only materials contain Au NPs have a peak at wavelength of 532 nm, otherwise no absorbance observed. Therefore, we could make sure that when irradiated by laser, the energy wouldn't decrease after travelling through the treatment solution since they don't absorb light.

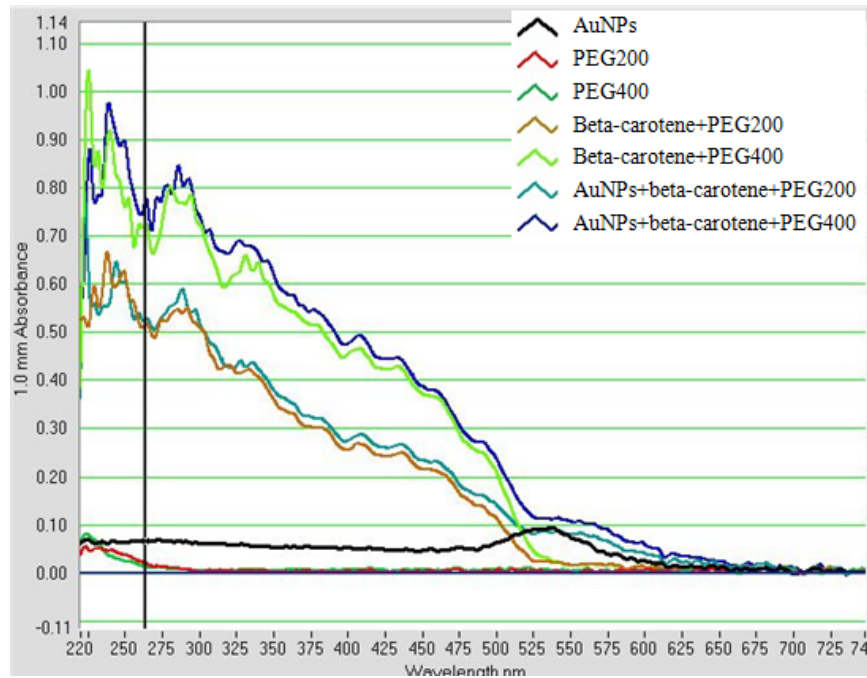


Figure 3.10 Absorbance of different kinds of materials at wavelength from 220 to 740 nm.

3.3.2 Impact of Cells with Membrane-bounded Au NPs Suspended in 1× PBS

Figure 3.11 shows the irradiated area of cells bounded with Au NPs and suspended only in 1× PBS. There are not a lot blue dots in the irradiated area. Dark region means that cells were alive. The cell death of this irradiated area was measured by imageJ with the average value of 1.31%. This excludes the possibility that PBS is toxic to cells.

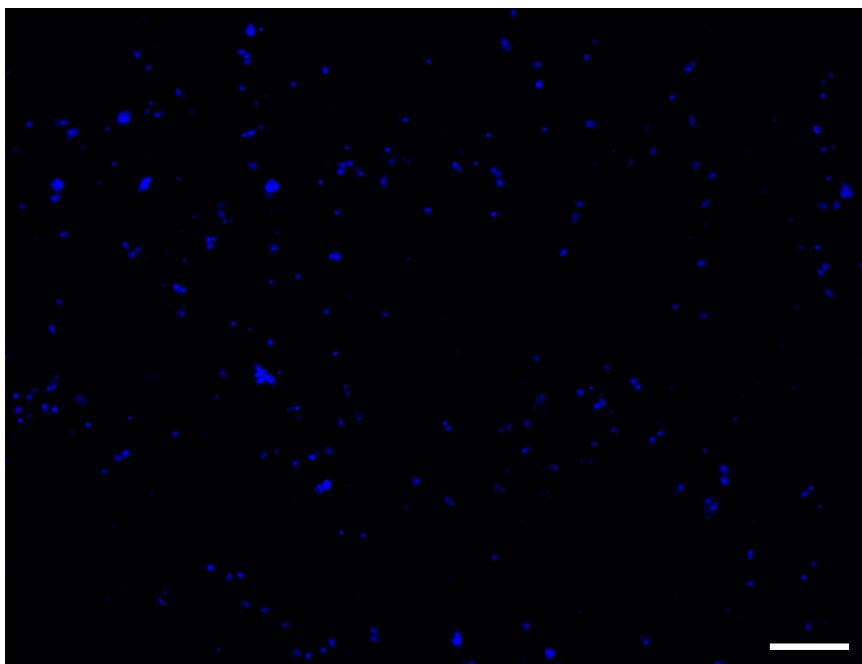


Figure 3.11 (Color online) Irradiated area of cells bounded with Au NPs suspended in 1× PBS. The blue fluorescence indicates dead cells. Scale bar is 200 μm .

3.3.3 Impact of Cells without Membrane-bounded Au NPs Suspended in PEG

Solutions

Figure 3.12 demonstrates the irradiated area of cells without membrane-bounded Au NPs and suspended in 20% PEG200 and 20% PEG400. Few blue dots can be seen in the pictures, which indicate that cells didn't die a lot. Cell death was measured with average value of 0.64% and standard deviation of 0.08% for 20% PEG200 and cell death of 0.65%

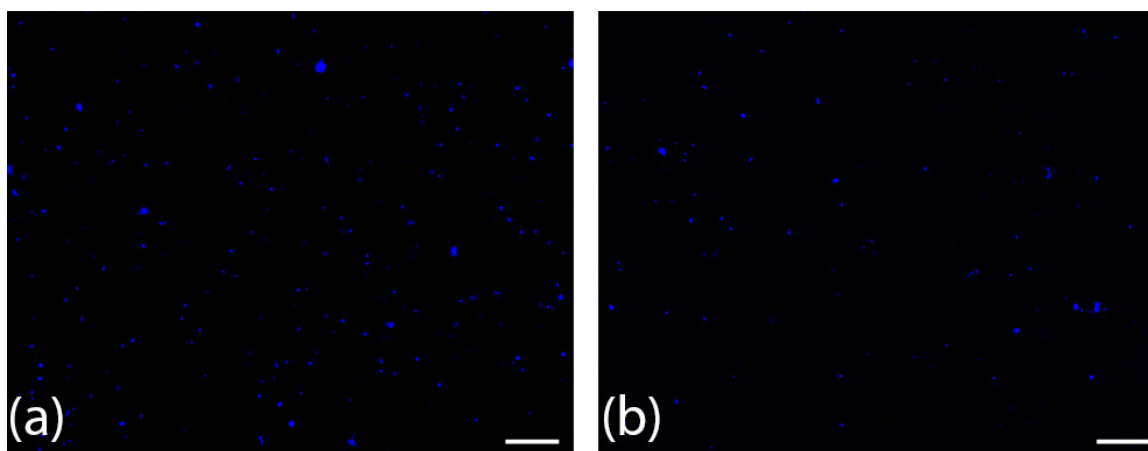


Figure 3.12 (Color online) Fluorescence images of irradiated cells without Au NPs suspended in (a) 20% PEG400, (b) 20% PEG200 under laser treatment. Blue dots indicate dead cells that internalized fluorescent dye. Scale bar is 200 μm .

with standard deviation of 0.12% for 20% PEG400. This phenomenon confirms that without Au NPs, heat cannot be generated during laser exposure. Hence, Au NPs played an important role in these experiments. ANOVA test ($\alpha=0.05$) on the cell death caused in those two conditions results that there is no essential difference between these two conditions, even though the dead cells look more in figure 3.12 (a) than in figure 3.12 (b).

3.4 Influence of β -Carotene/DPPC Liposomes on Irradiated Cells

As talked in the introduction section, β -carotene has influence on breast cancer cells. Since it is not water soluble, we made β -carotene/DPPC liposomes as treatment drugs. Result showed great cell non-viability as seen in figure 3.13. In this figure, we can see large amount of dead cells that are stained by Calcofluor white. Cell death was measured with the average value of 60.39%. This value is even bigger than at the condition of β -carotene/PEG solutions.

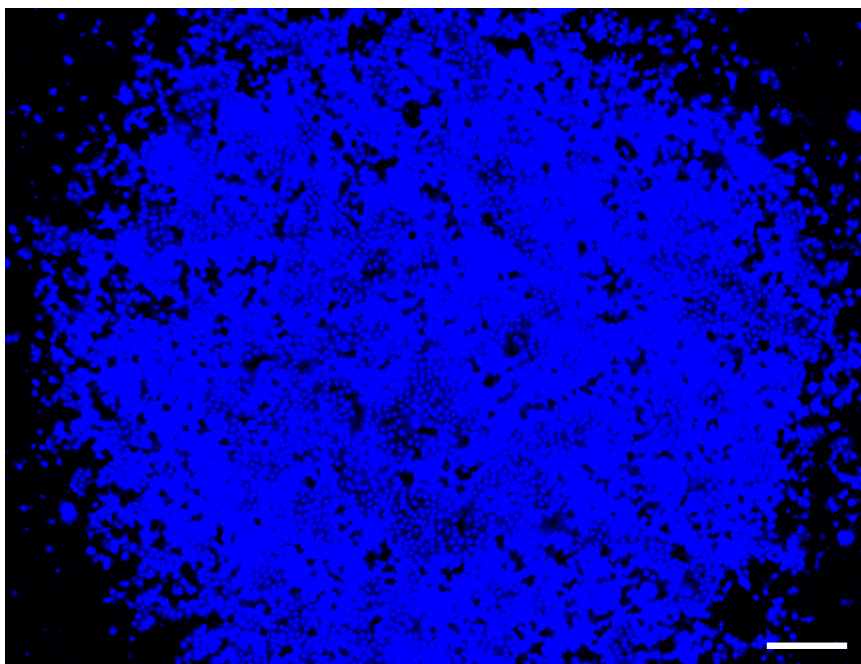


Figure 3.13 (Color online) Fluorescence image of large amount of cell death from β -carotene/DPPC liposomes in the irradiated region of the cell dish. The blue regions indicate dead cells. Scale bar is 200 μm .

3.5 Influence of Tetracycline on Irradiated Cells

When imaging under the fluorescence microscope, we found that many dead cells from some parts of the irradiated area were not stick to the dish wall. This should be due to the two hours incubation instead of half hour after laser treatment, even though trypan blue was chosen to dye the dead cells due to its short stain time. We got images as seen one of them in figure 3.14. This image can show clearly the irradiated region and the cell death was measured of 19.67% with standard deviation of 4.5%. Since it was long time incubation after the laser treatment, cell proliferation was affected and cells were washed away when cleaning by the $1 \times \text{PBS}$. This resulted in cell death with high standard deviation.

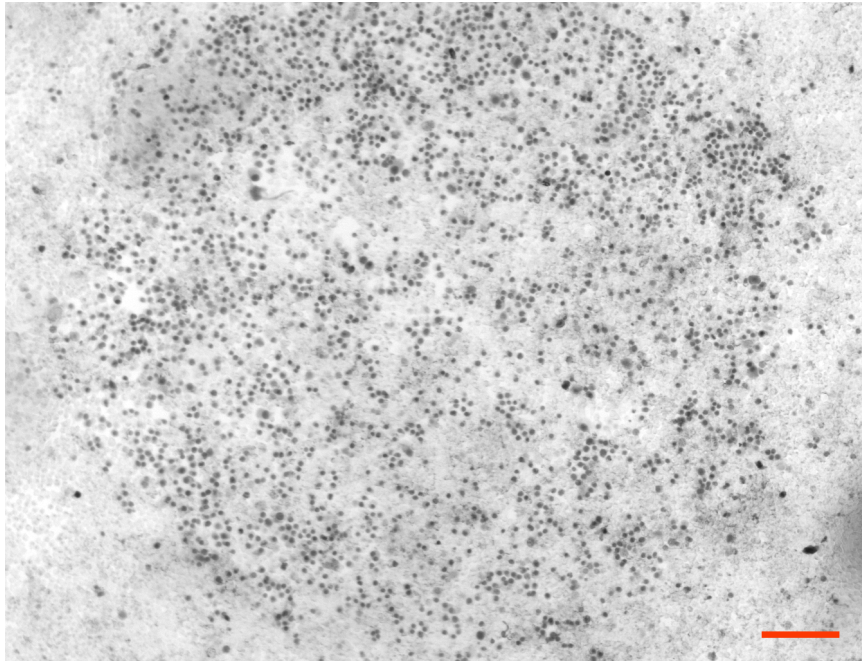


Figure 3.14 Image of irradiated cells suspended in tetracycline. Dark dots indicate dead cells, while others are living cells. Circle region is the irradiated region. Scale bar is 200 μm .

Chapter 4

Discussion

4.1 Comparison Between PEG200 and PEG400 in the Absence/Presence of β -Carotene

As shown before, we got large number of data. When comparing cell death resulted from PEG200 and PEG400 at the same concentration, we found that the percent of non-viable cells suspended in the same concentration of PEG200 and PEG400 are similar, as seen in figure 4.1. ANOVA test ($\alpha=0.1$) also proved that there is no essential difference between PEG200 and PEG400 when compared cell death at the same concentration.

In addition, comparison of PEG200 and PEG400 in the presence of β -carotene can

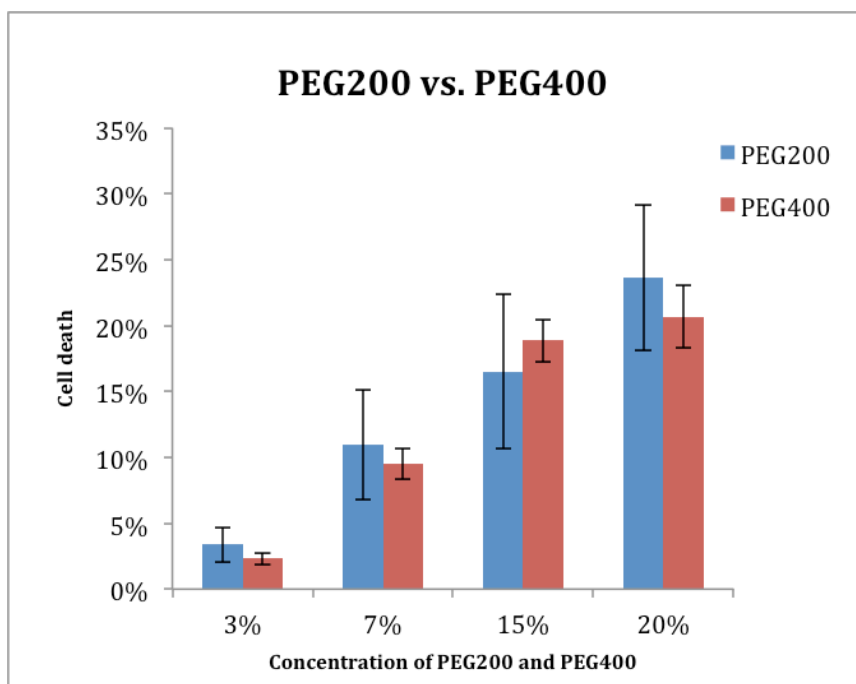


Figure 4.1 Comparison of cell death resulted from PEG200 and PEG400. The results show that there is no big difference between PEG200 and PEG400 when at the same concentration.

been seen in figure 4.2. ANOVA test ($\alpha=0.1$) on cell death results that there is also no big difference between β -carotene/PEG200 and β -carotene/PEG400 solutions at the same concentration.

Figure 4.3 shows the comparison of cell death resulted from β -carotene/ PEG200 and PEG200. In this figure we can see clearly that after laser treatment, cell non-viability caused by β -carotene/PEG200 is almost twice larger than by only PEG200 at the same concentration. ANOVA test ($\alpha=0.05$) shows that $p<0.05$, which proves that cell non-viability is much larger in β -carotene/PEG200 compared as PEG200 at the same concentration. Similarly, ANOVA test ($\alpha=0.05$) also confirms significantly different cell non-viability between β -carotene/PEG400 and PEG400 at the same concentration. As seen in figure 4.4, the percent of non-viable cells suspended in β -carotene/PEG400 is much larger than in only PEG400 at the same concentration.

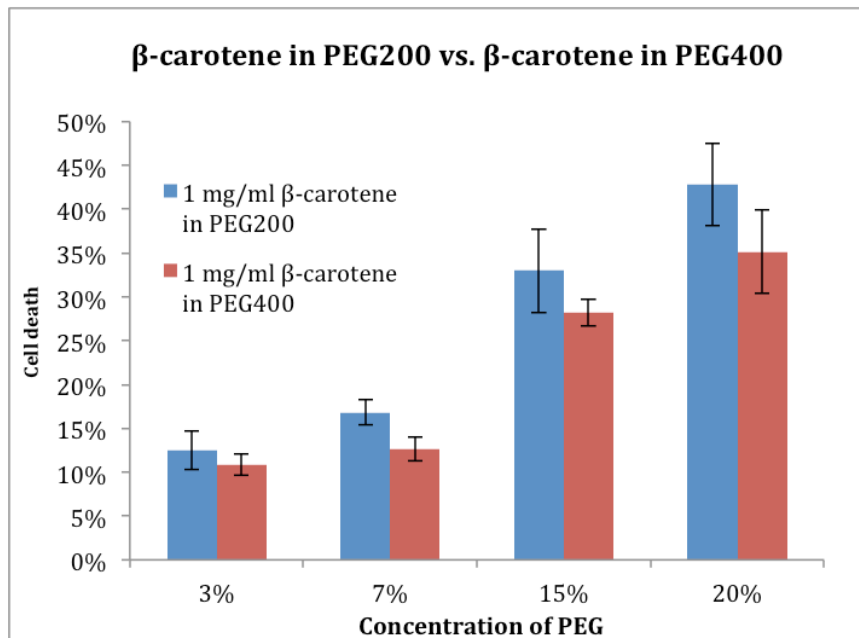


Figure 4.2 Comparison of cell death resulted from β -carotene/PEG200 and β -carotene/ PEG400. The results show that there is no big difference on cell death when at the same concentration.

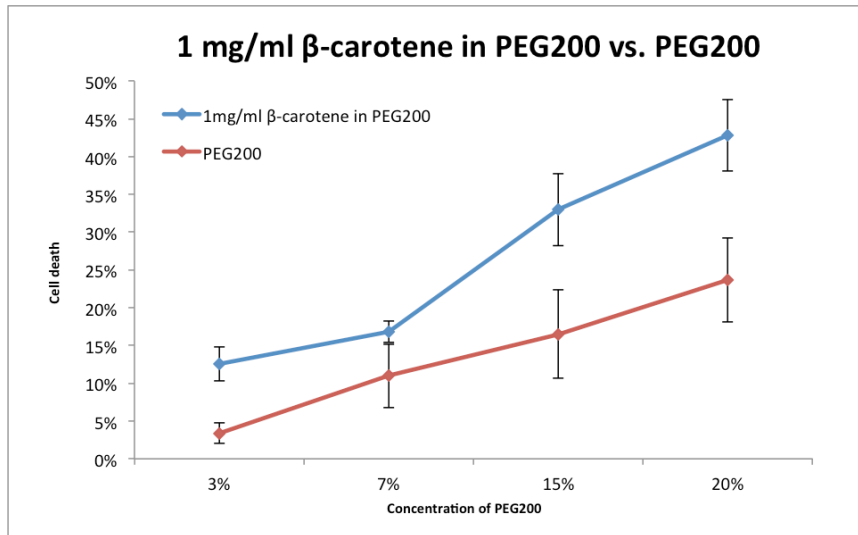


Figure 4.3 The plot shows the cell death caused by β -carotene/PEG200 is much larger than by PEG200 at respective concentration.

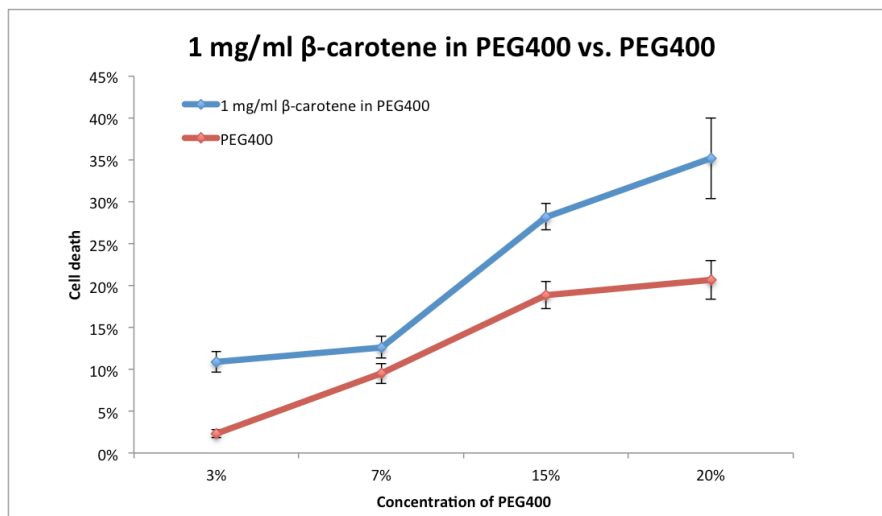


Figure 4.4 The plot shows the cell death caused by β -carotene/PEG200 is much larger than by PEG200 at respective concentration.

Generally, there is no difference between PEG200 and PEG400 as the anti-cancer drug or as the β -carotene dissolvent. Hemant et al indicated that PEG is a highly effective chemopreventive agent against colon cancer. They demonstrated that PEG treatment resulted in a dose- and time-dependent cell non-viability.⁵⁹ Other experiments have also run to prove this. Olga et al analyzed low weight PEG polymers and claimed a likely

conclusion that those molecules have fewer oxyethylene units, which resulted in clastogenic and cell apoptosis.⁶⁰ Another reason has been reported that after PEGs go into cells, high osmotic pressures will be generated and cells die from cell membrane blasts.⁶¹

On the other hand, even though both PEG200 and PEG400 can result in cell death along with laser treatment, cell death is much higher when β -carotene exists in PEG solutions. In other words, β -carotene has greater influence on T47D breast cancer cell proliferation. Additionally, figure 3.12 indicates that PBS has no damage to both irradiated and non-irradiated cells. Meanwhile, without Au NPs, heat cannot be generated to loosen the cell membrane and drugs cannot be delivered into cells to affect the cell proliferation.

4.2 β -Carotene/DPPC Liposomes as Anti-cancer Drug

Since β -carotene is barely water soluble, DPPC has been proved to be an effective delivery method with little influence on cell proliferation. As seen in figure 3.14, β -carotene/DPPC liposomes have great impact on breast cancer cell non-viability with a high cell death up to 65%, even higher than β -carotene/PEG solutions. This result confirms that β -carotene/DPPC liposomes can be a good anti-cancer drug along with laser treatment of 20 mJ/cm² for 20 seconds.

4.3 Tetracycline as Anti-cancer Drug

Even though tetracycline has proved to be an effective anti-cancer drug in many areas, it is not as effective as β -carotene in our research. Cell non-viability caused by

tetracycline is about 20% with a high standard deviation. As an anti-cancer drug, it is not as stable as β -carotene probably because of the long time interaction with cells. However, further studies are needed to discover tetracycline as anti-breast cancer drugs.

Chapter 5

Conclusion

Inspired by previous optoporation work, Au NPs can absorb electromagnetic radiation strongly and generate heat under illumination. Hence, we used laser with wavelength of 532 nm and energy of 20 mJ/cm² to heat the breast cancer cells, which have been attached with Au NPs. In this case, holes were generated on cell membrane so that anti-cancer drugs could go into the cells. The advantage of optoporation is that we can selectively kill the target cells by introducing laser to those target cells. Here, we used phytochemical β -carotene dissolved in PEG200 and PEG400 or β -carotene/DPPC liposomes as well as tetracycline as drugs. Results excluded the possibility that PBS has effect on cell proliferation. In the mean time, Au NPs has been proved to be necessary during laser treatment to absorb light to convert to heat and enable the generation of holes on cell membrane, which make large molecular drugs' delivery possible. Moreover, both PEG and β -carotene/PEG solutions result in cell death and cell death is higher when β -carotene exists. On the other hand, β -carotene/DPPC liposomes appear to be the best anti-cancer drugs in this study, with cell death up to 65%. We also ran experiments by using tetracycline as anti-cancer drug, but the cell death is only about 20% along with high standard deviation.

More phytochemicals such as lycopene and curcumin can be studied as anti-cancer drugs along with optoporation method in the future and hopefully it can be applied in clinic.

Appendix A

Calculation for Cell Death by ImageJ

Fluorescence images were taken under IX 70 Olympus microscope, as seen one of these images below. Figure A.1 is fluorescence image of cell death caused by 20% β -carotene/PEG200 along with laser treatment. We can see clearly that there is a circle area that contains most blue fluorescence. This area is the irradiated area. Converted this blue fluorescence image to a binary image by using imageJ, which means blue fluorescence would turn into black, black area would turn into white area. Then selected the irradiated area, we got the count of black pixel, the count of white pixel and total count through imageJ. Here we determined cell death equals the count of black pixel (dead cells) divided by total count (total irradiated), we got the cell death of each fluorescence image.

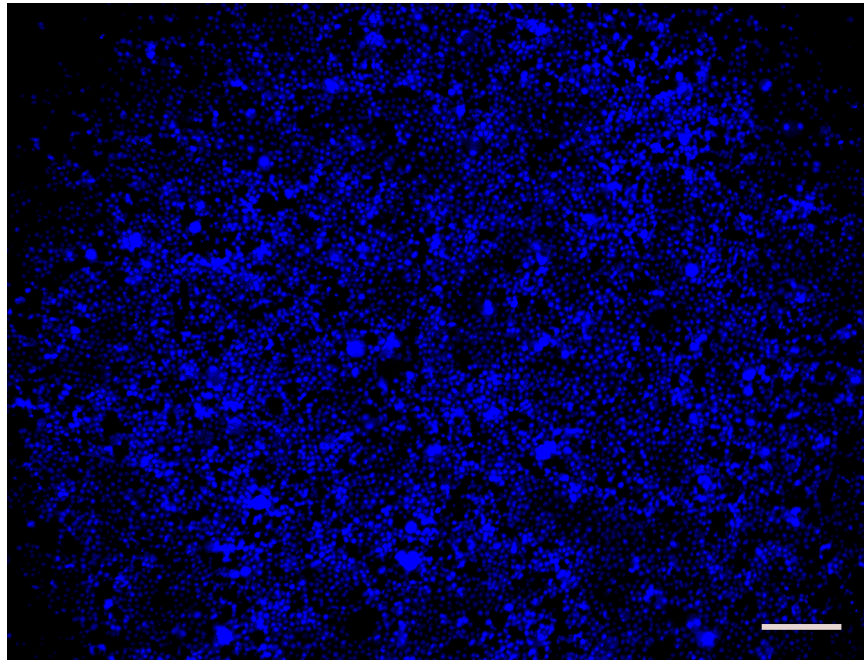


Figure A.1 (Color online) Fluorescence image of non-viable cells suspended in 20% β -carotene/PEG200 solution. Scale bar is 200 μm .

BIBLIOGRAPHY

1. Alteri, R., Bandi, P., Brinton, L., Casares, C. & Cokkinides, V. (2011). Breast cancer facts and figures 2011–2012. *Atlanta: American Cancer Society, Inc.*
2. Davies, E. L. (2012). Breast cancer. *Medicine* **40**, 5-9.
3. Schratte-Sehn, A. U. (2012). Breast cancer radiotherapy. *HAMDAN MEDICAL JOURNAL* **5**, 51–56.
4. CTSU, R. I. (2005). Effects of chemotherapy and hormonal therapy for early breast cancer on recurrence and 15-year survival: an overview of the randomised trials. *Lancet* **365**, 1687-1717.
5. Sporn, M., Dunlop, N., Newton, D. & Smith, J. (1976). *Federation proceedings*.
6. Johnson, S. M., Wang, X. & Evers, B. M. (2011). Triptolide inhibits proliferation and migration of colon cancer cells by inhibition of cell cycle regulators and cytokine receptors. *Journal of Surgical Research* **168**, 197-205.
7. Surh, Y.-J. (2003). Cancer chemoprevention with dietary phytochemicals. *Nature Reviews Cancer* **3**, 768-780.
8. Johnson, I. T. (2007). Phytochemicals and cancer. *Proceedings of the Nutrition Society* **66**, 207-215.
9. Shu, L., Cheung, K.-L., Khor, T. O., Chen, C. & Kong, A.-N. (2010). Phytochemicals: cancer chemoprevention and suppression of tumor onset and metastasis. *Cancer and Metastasis Reviews* **29**, 483-502.
10. Ziegler, R. G. (1989). A review of epidemiologic evidence that carotenoids reduce the risk of cancer. *The Journal of nutrition* **119**, 116-122.
11. Bertram, J. S., Pung, A., Churley, M., Kappock, T. J., Wilkins, L. R. & Cooney, R. V. (1991). Diverse carotenoids protect against chemically induced neoplastic transformation. *Carcinogenesis* **12**, 671-678.
12. Rohan, T. E., Howe, G. R., Friedenreich, C. M., Jain, M. & Miller, A. B. (1993). Dietary fiber, vitamins A, C, and E, and risk of breast cancer: a cohort study. *Cancer Causes & Control* **4**, 29-37.
13. Verhoeven, D., Assen, N., Goldbohm, R., Dorant, E., Van'T Veer, P., Sturmans, F., Hermus, R. & Van den Brandt, P. (1997). Vitamins C and E, retinol, beta-carotene and dietary fibre in relation to breast cancer risk: a prospective cohort study. *British journal of cancer* **75**, 149.

14. Toniolo, P., Van Kappel, A. L., Akhmedkhanov, A., Ferrari, P., Kato, I., Shore, R. E. & Riboli, E. (2001). Serum carotenoids and breast cancer. *American Journal of Epidemiology* **153**, 1142-1147.
15. Hu, X., White, K. M., Jacobsen, N. E., Mangelsdorf, D. J. & Canfield, L. M. (1998). Inhibition of growth and cholesterol synthesis in breast cancer cells by oxidation products of β -carotene. *The Journal of Nutritional Biochemistry* **9**, 567-574.
16. Tanvetyanon, T. & Bepler, G. (2008). Beta-carotene in multivitamins and the possible risk of lung cancer among smokers versus former smokers. *Cancer* **113**, 150-157.
17. Carballoso, M., Sacristan, M., Serra, C. & Bonfill, X. (2003). Drugs for preventing lung cancer in healthy people. *Cochrane Database Syst Rev* **2**.
18. Wang, X.-D., Russell, R. M., Marini, R. P., Tang, G., Dolnikowski, G. G., Fox, J. G. & Krinsky, N. I. (1993). Intestinal perfusion of β -carotene in the ferret raises retinoic acid level in portal blood. *Biochimica et Biophysica Acta (BBA)-Lipids and Lipid Metabolism* **1167**, 159-164.
19. Russell, R. M. (2002). Beta-carotene and lung cancer. *Pure and applied chemistry* **74**, 1461-1467.
20. Rao, A. V. & Agarwal, S. (2000). Role of antioxidant lycopene in cancer and heart disease. *Journal of the American College of Nutrition* **19**, 563-569.
21. Nagasawa, H., Mitamura, T., Sakamoto, S. & Yamamoto, K. (1994). Effects of lycopene on spontaneous mammary tumour development in SHN virgin mice. *Anticancer research* **15**, 1173-1178.
22. Hieber, A. D., King, T. J., Morioka, S., Fukushima, L. H., Franke, A. A. & Bertram, J. S. (1999). Comparative effects of all-trans beta-carotene vs. 9-cis beta-carotene on carcinogen-induced neoplastic transformation and connexin 43 expression in murine 10T1/2 cells and on the differentiation of human keratinocytes. *Nutrition and cancer* **37**, 234-244.
23. Fornelli, F., Leone, A., Verdesca, I., Minervini, F. & Zacheo, G. (2007). The influence of lycopene on the proliferation of human breast cell line (MCF-7). *Toxicology in vitro* **21**, 217-223.
24. Tang, L., Jin, T., Zeng, X. & Wang, J.-S. (2005). Lycopene inhibits the growth of human androgen-independent prostate cancer cells in vitro and in BALB/c nude mice. *The Journal of nutrition* **135**, 287-290.

25. Salman, H., Bergman, M., Djaldetti, M. & Bessler, H. (2007). Lycopene affects proliferation and apoptosis of four malignant cell lines. *Biomedicine & pharmacotherapy* **61**, 366-369.
26. Chattopadhyay, I., Biswas, K., Bandyopadhyay, U. & Banerjee, R. K. (2004). Turmeric and curcumin: Biological actions and medicinal applications. *Current science* **87**, 44-53.
27. Sharma, R., Gescher, A. & Steward, W. (2005). Curcumin: the story so far. *European Journal of Cancer* **41**, 1955-1968.
28. Shao, Z. M., Shen, Z. Z., Liu, C. H., Sartippour, M. R., Go, V. L., Heber, D. & Nguyen, M. (2002). Curcumin exerts multiple suppressive effects on human breast carcinoma cells. *International Journal of Cancer* **98**, 234-240.
29. Kunnumakkara, A. B., Anand, P. & Aggarwal, B. B. (2008). Curcumin inhibits proliferation, invasion, angiogenesis and metastasis of different cancers through interaction with multiple cell signaling proteins. *Cancer letters* **269**, 199-225.
30. Carroll, C. E., Ellersieck, M. R. & Hyder, S. M. (2008). Curcumin inhibits MPA-induced secretion of VEGF from T47-D human breast cancer cells. *Menopause* **15**, 570-574.
31. Nagaraju, G. P., Aliya, S., Zafar, S. F., Basha, R., Diaz, R. & El-Rayes, B. F. (2012). The impact of curcumin on breast cancer. *Integrative Biology* **4**, 996-1007.
32. Mehta, K., Pantazis, P., McQueen, T. & Aggarwal, B. B. (1997). Antiproliferative effect of curcumin (diferuloylmethane) against human breast tumor cell lines. *Anti-cancer drugs* **8**, 470-481.
33. Song, F., Zhang, L., Yu, H.-X., Lu, R.-R., Bao, J.-D., Tan, C. & Sun, Z. (2012). The mechanism underlying proliferation-inhibitory and apoptosis-inducing effects of curcumin on papillary thyroid cancer cells. *Food Chemistry* **132**, 43-50.
34. Watson, J. L., Hill, R., Lee, P. W., Giacomantonio, C. A. & Hoskin, D. W. (2008). Curcumin induces apoptosis in HCT-116 human colon cancer cells in a p21-independent manner. *Experimental and molecular pathology* **84**, 230-233.
35. Stevenson, D. J., Gunn-Moore, F. J., Campbell, P. & Dholakia, K. (2010). Single cell optical transfection. *Journal of the Royal Society Interface* **7**, 863-871.
36. Greulich, K. O. (1999). Micromanipulation by light in biology and medicine.
37. Mohanty, S. K., Sharma, M. & Gupta, P. K. (2003). Laser-assisted microinjection into targeted animal cells. *Biotechnology letters* **25**, 895-899.

38. Lei, M., Xu, H., Yang, H. & Yao, B. (2008). Femtosecond laser-assisted microinjection into living neurons. *Journal of neuroscience methods* **174**, 215-218.
39. Bhattacharyya, K. (2013). Detection of circulating breast cancer cells using photoacoustic flow cytometry, University of Missouri--Columbia.
40. Soughayer, J. S., Krasieva, T., Jacobson, S. C., Ramsey, J. M., Tromberg, B. J. & Allbritton, N. L. (2000). Characterization of cellular optoporation with distance. *Analytical chemistry* **72**, 1342-1347.
41. Schneckenburger, H., Hendinger, A., Sailer, R., Schmitt, M. & Strauss, W. S. (2002). Laser-assisted optoporation of single cells. *Journal of biomedical optics* **7**, 410-416.
42. Zhou, Y., Zhou, X.-Y., Wang, Z.-G., Zhu, Y.-F. & Li, P. (2010). Elevation of plasma membrane permeability upon laser irradiation of extracellular microbubbles. *Lasers in medical science* **25**, 587-594.
43. Praveen, B. B., Stevenson, D. J., Antkowiak, M., Dholakia, K. & Gunn-Moore, F. J. (2011). Enhancement and optimization of plasmid expression in femtosecond optical transfection. *Journal of biophotonics* **4**, 229-235.
44. He, H., Kong, S.-K., Lee, R. K.-Y., Suen, Y.-K. & Chan, K. T. (2008). Targeted photoporation and transfection in human HepG2 cells by a fiber femtosecond laser at 1554 nm. *Optics letters* **33**, 2961-2963.
45. Chen, H., McGrath, T. & Diebold, G. J. (1997). Laser chemistry in suspensions: new products and unique reaction conditions for the carbon–steam reaction. *Angewandte Chemie International Edition in English* **36**, 163-166.
46. Löwen, H. & Madden, P. A. (1992). A microscopic mechanism for shock-wave generation in pulsed-laser-heated colloidal suspensions. *The Journal of chemical physics* **97**, 8760-8766.
47. Chakravarty, P., Qian, W., El-Sayed, M. A. & Prausnitz, M. R. (2010). Delivery of molecules into cells using carbon nanoparticles activated by femtosecond laser pulses. *Nature nanotechnology* **5**, 607-611.
48. Giljohann, D. A., Seferos, D. S., Daniel, W. L., Massich, M. D., Patel, P. C. & Mirkin, C. A. (2010). Gold nanoparticles for biology and medicine. *Angewandte Chemie International Edition* **49**, 3280-3294.
49. Namura, K., Suzuki, M., Nakajima, K. & Kimura, K. (2011). Heat-generating property of a local plasmon resonator under illumination. *Optics letters* **36**, 3533-3535.

50. Yao, C., Qu, X., Zhang, Z., Hüttmann, G. & Rahmanzadeh, R. (2009). Influence of laser parameters on nanoparticle-induced membrane permeabilization. *Journal of biomedical optics* **14**, 054034-054034-7.
51. Sassaroli, E., Li, K. & O'Neill, B. (2009). Numerical investigation of heating of a gold nanoparticle and the surrounding microenvironment by nanosecond laser pulses for nanomedicine applications. *Physics in medicine and biology* **54**, 5541.
52. Bhattacharyya, K., Mehta, S. & Viator, J. (2012). Optically absorbing nanoparticle mediated cell membrane permeabilization. *Optics letters* **37**, 4474-4476.
53. Marttila, A. T., Laitinen, O. H., Airene, K. J., Kulik, T., Bayer, E. A., Wilchek, M. & Kulomaa, M. S. (2000). Recombinant NeutraLite avidin: a non-glycosylated, acidic mutant of chicken avidin that exhibits high affinity for biotin and low non-specific binding properties. *FEBS letters* **467**, 31-36.
54. van der Gun, B. T., Melchers, L. J., Ruiters, M. H., de Leij, L. F., McLaughlin, P. M. & Rots, M. G. (2010). EpCAM in carcinogenesis: the good, the bad or the ugly. *Carcinogenesis* **31**, 1913-1921.
55. Fischer, J. M., Peterson, C. A. & Bols, N. (1985). A new fluorescent test for cell vitality using calcofluor white M2R. *Biotechnic & Histochemistry* **60**, 69-79.
56. Baranowitz, S. A. (2005). Systemic formulations containing beta-carotene and derivatives thereof. Google Patents.
57. Stivala, L. A., Savio, M., Cazzalini, O., Pizzala, R., Rehak, L., Bianchi, L., Vannini, V. & Prospero, E. (1996). Effect of β -carotene on cell cycle progression of human fibroblasts. *Carcinogenesis* **17**, 2395-2401.
58. Connell, S. R., Tracz, D. M., Nierhaus, K. H. & Taylor, D. E. (2003). Ribosomal protection proteins and their mechanism of tetracycline resistance. *Antimicrobial agents and chemotherapy* **47**, 3675-3681.
59. Roy, H. K., DiBaise, J. K., Black, J., Karolski, W. J., Ratashak, A. & Ansari, S. (2001). Polyethylene glycol induces apoptosis in HT-29 cells: potential mechanism for chemoprevention of colon cancer. *FEBS letters* **496**, 143-146.
60. Biondi, O., Motta, S. & Mosesso, P. (2002). Low molecular weight polyethylene glycol induces chromosome aberrations in Chinese hamster cells cultured in vitro. *Mutagenesis* **17**, 261-264.
61. Money, N. P. (1989). Osmotic pressure of aqueous polyethylene glycols relationship between molecular weight and vapor pressure deficit. *Plant physiology* **91**, 766-769.

VITA

Feifei was born in Yangzhou city, Jiangsu Providence, China on June 9th, 1990. She finished her primary education in Yangzhou and finished her undergraduate studies with a degree in Biological Engineering at Shanghai University in Shanghai, China in 2012. She has been in America for two and a half years since year 2012 for the degree of Master of Science of Bioengineering in University of Missouri.